Traveling wave solutions of a highly nonlinear shallow water equation

Geyer, Anna; Quirchmayr, Ronald

DOI
10.3934/dcds.2018065

Publication date
2018

Document Version
Final published version

Published in
Discrete and Continuous Dynamical Systems A

DISCRETE AND CONTINUOUS
DYNAMICAL SYSTEMS
Volume **38**, Number **3**, March **2018**

doi:10.3934/dcds.2018065

pp. **1567–1604**

TRAVELING WAVE SOLUTIONS OF A HIGHLY NONLINEAR SHALLOW WATER EQUATION

Anna Geyer*

Delft University of Technology
Delft Institute of Applied Mathematics, Faculty of EEMCS
Mekelweg 4, 2628 CD Delft, The Netherlands

Ronald Quirchmayr

KTH Royal Institute of Technology
Department of Mathematics
Lindstedtsvägen 25, 100 44 Stockholm, Sweden

(Communicated by Adrian Constantin)

Abstract. Motivated by the question whether higher-order nonlinear model equations, which go beyond the Camassa-Holm regime of moderate amplitude waves, could point us to new types of waves profiles, we study the traveling wave solutions of a quasilinear evolution equation which models the propagation of shallow water waves of large amplitude. The aim of this paper is a complete classification of its traveling wave solutions. Apart from symmetric smooth, peaked and cusped solitary and periodic traveling waves, whose existence is well-known for moderate amplitude equations like Camassa-Holm, we obtain entirely new types of singular traveling waves: periodic waves which exhibit singularities on both crests and troughs simultaneously, waves with asymmetric peaks, as well as multi-crested smooth and multi-peaked waves with decay. Our approach uses qualitative tools for dynamical systems and methods for integrable planar systems.

1. **Introduction.** Recent research literature shows strong interest in the study of singular traveling waves for model equations in hydrodynamics. On the one hand, the governing equations for water waves admit the celebrated Stokes waves of greatest height, see the discussions in [5, 34, 39, 38]. Moreover, cusped traveling waves are also known to occur as solutions to the governing equations for water waves [6, 7, 23]. These types of solutions are real-analytic except at their peaked or cusped crests, which are points of stagnation. We note that traveling waves in irrotational flows without stagnation points are real-analytic everywhere, in the periodic as well as in the solitary case, see the discussion in the papers [9, 25]. On the other hand, singular traveling wave solutions involving peaks and cusps are encountered in the study of shallow water approximations. While weakly nonlinear model equations for small amplitude waves, like the Korteweg-de-Vries equation (KdV), do not capture these

2010 *Mathematics Subject Classification.* Primary: 35Q35, 58F17; Secondary: 34C37.

Key words and phrases. Shallow water equation, traveling waves, phase plane analysis.

A. Geyer acknowledges the support of the Austrian Science Fund (FWF) project J3452 "Dynamical Systems Methods in Hydrodynamics". R. Quirchmayr acknowledges the support of the Austrian Science Fund (FWF), Grant W1245.

* Corresponding author: Anna Geyer.

phenomena, peaked or cusped solutions do arise from model equations for waves of moderate amplitude, like the Camassa-Holm equation (CH) and Degasperis-Procesi equation (DP) [4, 31, 32]. This raises the question whether higher-order nonlinear model equations, which go beyond the regime of moderate amplitude waves, could point us to other, new types of singular traveling waves. In this paper we give an affirmative answer to this question. A natural candidate for such a new type of wave is one which exhibits singularities on both the crest and the trough of the wave simultaneously. Model equations for moderate amplitude waves do not possess this type of singular solutions, since their nonlinearities in the higher order terms are at most quadratic. In this paper we study the traveling wave solutions of the following new model equation, which encompasses stronger nonlinearities to allow for new types of singular solutions:

$$u_t+u_x+\frac{3}{2}uu_x-\frac{4}{18}u_{xxx}-\frac{7}{18}u_{xxt}=\frac{1}{12}(u_x^2+2uu_{xx})_x-\frac{1}{96}(45u^2u_{xx}+154uu_x^2)_x. \quad (1)$$

Here, the dependent variable $u=u(x,t)$ is a function of one spatial variable $x\in\mathbb{R}$ and the time variable $t>0$. The solutions of this equation describe the evolution of the horizontal velocity component of a flow field at a certain fixed depth beneath the free surface of a water wave propagating unidirectionally over a flat bed. This equation was derived in [35] in the spirit of [26] from the incompressible Euler equations for gravity water waves using double asymptotic expansions in the two fundamental water wave parameters: δ, the shallowness parameter, and ε, the amplitude parameter. In this terminology, equation (1) is a model for gravity water waves in the regime characterized by $\delta\ll 1, \varepsilon=O(\sqrt{\delta})$ which we call *the shallow water regime for large amplitude waves*, see [35]. This regime allows for the description of large amplitude waves whose strong nonlinear effects are captured by the cubic terms on the right hand side. For convenience we have scaled out the parameters δ and ε to write the equation in the form (1).

It is well-known that weakly nonlinear models for shallow water waves of *small amplitude*, i.e. $\varepsilon=O(\delta^2)$, such as the KdV [27], admit smooth solitary and periodic traveling waves. Shallow water models for waves of *moderate amplitude*, i.e. $\varepsilon=O(\delta)$, such as the CH [4], the corresponding equation for free surface waves [8, 10, 26] as well as the DP [15], capture stronger nonlinear effects and admit also non-smooth solutions containing so-called peaks and cusps, see for instance [21, 31, 32]. For the present equation we discover entirely new kinds of traveling wave solutions, which are not governed by equations for moderate amplitude waves. In Fig. 1 we sketch the shapes of some of these waves in order to give the reader a first impression of the tremendously rich collection of traveling wave solutions of (1). Novel types of solutions include periodic waves with peaks both at the crests and the troughs, as well as multi-crested smooth and peaked solitary waves. Another interesting feature of equation (1) is that it allows for peaked solutions with different slopes on either side of the crest and trough, that is, we obtain non-symmetric peakons. In comparison, peaks are always symmetric in CH type equations, cf. [31]. Moreover, equation (1) admits peaked and cusped solutions with compact support, which was shown to be impossible for CH type equations in [21]. As we will see, the existence of such solutions requires the presence of third order terms exhibiting nonlinearities of at least cubic order in the evolution equation.

The aim of this paper is to give a complete classification of all traveling wave solutions of (1) in H^1_{loc}, where a suitable weak formulation of the evolution equation is available. Our approach relies on methods from the qualitative theory of dynamical

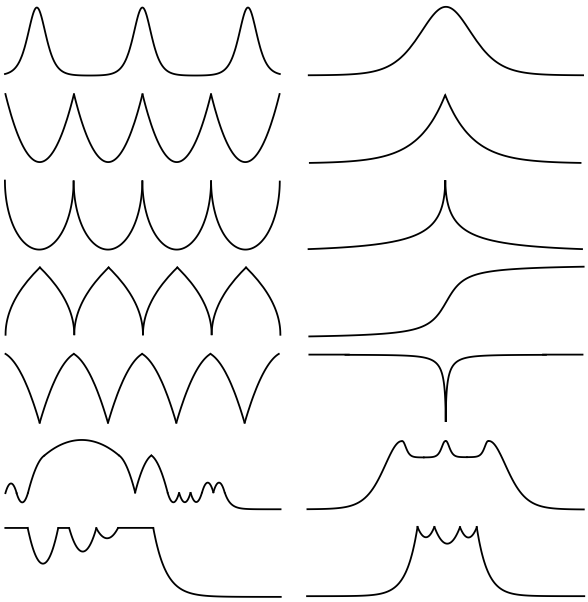

FIGURE 1. A selection of some traveling wave solutions of (1). The waves on the left side from top to bottom are of the following types: smooth periodic, peaked periodic, cusped periodic, periodic with peaked crests and cusped troughs, periodic with peaked crests and troughs, composite, composite with plateaus. Right side top to bottom: smooth solitary, peaked solitary, cusped solitary, wavefront, compactly supported anticusp, multi-crest with decay, multi-peak with decay.

systems, in particular on tools for integrable planar systems. In contrast to prominent moderate amplitude shallow water models like CH and DP, the traveling wave equation corresponding to (1) does *not* give rise to a Hamiltonian planar system. Instead our analysis is based on the existence of a non-explicit first integral with a singular integrating factor, cf. (13). Working with a suitable weak formulation we will describe precisely in which sense such non-smooth traveling waves are solutions of equation (1).

The paper is structured as follows. In Section 2 we provide the definition of traveling wave solutions based on a weak formulation of (1). Section 3 discusses the integrable structure of the planar dynamical system associated to (1). In Section 4 we prove a proposition, which characterizes the traveling wave solutions as certain piecewise smooth H^1_{loc}-functions solving the aforementioned system almost everywhere in the classical sense. This opens the way to a full classification of all traveling wave solutions of (1) by means of a systematic phase plane analysis of a bi-parametric family of underlying dynamical systems. The construction of all possible traveling waves is finally realized in Section 5. We provide a summary of the results of our analysis in Theorems 6.1, 6.2 and 6.3 in Section 6 and conclude with a short discussion and outlook in Section 7.

2. **Weak formulation for traveling wave solutions.** In the current section, we give the definition of a traveling wave solution of (1), which is based on a weak formulation. Let us therefore assume that a function u solves (1) pointwise and satisfies the relation

$$u(t,x) = u(x-ct) \tag{2}$$

for a fixed $c \in \mathbb{R}$ being referred to as the *wave speed*. We denote by $s := x - ct$ the corresponding independent *moving frame variable*. In a first step, we rewrite (1) in the moving frame variables (2) and integrate with respect to the moving frame variable s to obtain

$$u''(A_c + Bu + Cu^2) = K + (c-1)u + Eu^2 + (u')^2(Gu - 1/2\,B), \tag{3}$$

where the prime symbol denotes differentiation with respect to s and

$$A_c = \frac{7c-4}{18}, \quad B = -\frac{1}{6}, \quad C = \frac{45}{96}, \quad E = -\frac{3}{4}, \quad G = -\frac{154}{96},$$

and $K \in \mathbb{R}$ is a constant of integration. To facilitate the mathematical treatment of this equation, let us introduce the real polynomials

$$\begin{aligned} g(u) &:= (A_c + Bu + Cu^2), \\ f(u,v) &:= K + (c-1)u + Eu^2 + v^2(Gu - 1/2\,B) \end{aligned} \tag{4}$$

and write equation (3) as

$$u''g(u) = f(u,u') \tag{5}$$

in a more compact form. An equivalent formulation which turns out to be convenient when working with H^1_{loc}-functions is

$$f(u,u') + (u')^2 g'(u) = [g(u)u']', \tag{6}$$

where $g'(u) = \frac{\mathrm{d}g}{\mathrm{d}u}(u)$, see Remark 2.2. The weak formulation of (1) suitable for functions u of the form (2) is then obtained by multiplying (6) with a smooth and compactly supported test function ϕ satisfying $\phi(t,x) = \phi(x-ct) = \phi(s)$ and by a subsequent integration over $\mathbb{R}$ with respect to the moving frame variable s.

Definition 2.1. Fix $c \in \mathbb{R}$. A bounded function $u\colon \mathbb{R} \to \mathbb{R}$ is called a *traveling wave solution*, or shorter, a *traveling wave* of (1) with wave speed c, if $u = u(s)$ lies in $H^1_{\mathrm{loc}}(\mathbb{R})$ and satisfies equation (6) in the sense of distributions, i.e. it satisfies

$$\int_{\mathbb{R}} g(u)u'\phi' + [f(u,u') + (u')^2 g'(u)]\phi \,\mathrm{d}s = 0 \tag{7}$$

for all test functions ϕ in $\mathcal{D}(\mathbb{R}) = \mathcal{C}^\infty_{\mathrm{c}}(\mathbb{R})$, the space of compactly supported smooth real-valued functions on $\mathbb{R}$.

Remark 2.2. We point out that, by abuse of notation, we write $g'(u)$ to mean $\frac{\mathrm{d}g}{\mathrm{d}u}(u)$. Moreover, when speaking of an element $u \in H^1_{\mathrm{loc}}(\mathbb{R})$, we always refer to the absolutely continuous representative of this class of functions. Hence a traveling wave of (1) is absolutely continuous and bounded with a locally square integrable derivative. Definition 2.1 excludes unbounded waves, which would not be relevant from a physical point of view.

Remark 2.3. Note that the weak formulation of (1) as given in Definition 2.1 applies exclusively to functions of the form (2), since the test functions ϕ that we consider are also of that form, and hence this weak formulation is not suitable for a general formulation of the Cauchy problem that corresponds to (1).

3. **The associated integrable planar system.** Our aim is to completely characterize all traveling wave solutions of (1). To this end, we study the phase portrait of the related planar differential system

$$\begin{cases} u' = v \\ v' = \dfrac{f(u,v)}{g(u)} \end{cases} \tag{8}$$

for all parameter pairs $(c, K) \in \mathbb{R}^2$. In Section 4 we will prove that this is sufficient since every traveling wave of (1) is a composition of solution curves of (8), cf. Proposition 4.1.

Let us first introduce some useful notation. We denote by N_g the set of real zeros of the polynomial $g(u)$, that is,

$$N_g := \{u \in \mathbb{R} \colon g(u) = 0\}, \tag{9}$$

and we denote by U the domain of system (8), i.e.

$$U := \mathbb{R}^2 \setminus (N_g \times \mathbb{R}). \tag{10}$$

Our analysis relies heavily on the fact, that (8) is integrable, i.e. there exists a function $H \colon U \to \mathbb{R}$, called *first integral*, which is constant along solution curves of (8) within the open subset $U \subseteq \mathbb{R}^2$. In order to find a first integral, we reparametrize system (8) by introducing the new independent variable τ via $\frac{\mathrm{d}s}{\mathrm{d}\tau} = g(u)$ to obtain

$$\begin{cases} \dot{u} = v\, g(u) \\ \dot{v} = f(u,v). \end{cases} \tag{11}$$

Note that (11) is defined on all of $\mathbb{R}^2$. The dots in (11) refer to differentiation with respect to τ. System (11) is topologically equivalent to system (8) on U: the solution curves coincide, but the orientation is reversed within the region $\{(u,v) \in U : g(u) < 0\}$ and preserved in $\{(u,v) \in U : g(u) > 0\}$, cf. [16, 22]. The set $N_g \times \mathbb{R} \subseteq \mathbb{R}^2$ is either empty, or consists of up to two vertical invariant lines.

System (11) has an integrating factor $\varphi \colon \mathbb{R} \setminus N_g \to \mathbb{R}$, i.e.

$$\operatorname{div}\left(vg(u)\varphi(u), f(u,v)\varphi(u)\right) = 0 \quad \text{in } U.$$

It is not difficult to see that if φ satisfies the differential equation

$$\varphi'(u) = -2(C+G)\frac{u}{g(u)}\varphi(u), \tag{12}$$

then φ is an integrating factor on $\mathbb{R} \setminus N_g$. Equation (12) can be solved explicitly and the form of the solution φ depends on the number of roots of the polynomial g; see Section 5.2 for the details. Hence (11) is integrable on U and the first integral H associated to the integrating factor φ is given by

$$H(u,v) := \frac{v^2}{2}\varphi(u)g(u) + \psi(u), \tag{13}$$

where

$$\psi(u) = -\int f_0(u)\varphi(u)\,\mathrm{d}u, \tag{14}$$

with $f_0(u) := f(u,0)$. Note that $\dot{u} = \frac{H_v}{\varphi(u)}, \dot{v} = -\frac{H_u}{\varphi(u)}$ in U. The solution curves, or *orbits*, of system (11) correspond to the level sets of H, which we denote by

$$L_h(H) := \{(u,v) \in U \colon H(u,v) = h\}. \tag{15}$$

In view of the symmetry of H about the u-axis, these curves are composed of the two symmetric branches $(u, v_h^{\pm}(u))$, where

$$v_h^{\pm}(u) = \pm\sqrt{2\frac{h-\psi(u)}{g(u)\varphi(u)}}. \tag{16}$$

Let us finally note that

$$\frac{\mathrm{d}u}{\mathrm{d}s} = v_h^{\pm} \quad \text{along solution curves of (8) in } U \cap (\mathbb{R}\times\mathbb{R}^{\pm}). \tag{17}$$

4. **A characterization of traveling wave solutions.** We will construct traveling wave solutions of (1) by associating the solutions of (5) with orbits of the planar systems (8) and (11). These orbits correspond to level sets of the first integral (13). The following proposition ensures that we can indeed obtain all traveling wave solutions of (1) with this approach.

Recall that N_g denotes the zero set of the quadratic polynomial g defined in (4). Moreover, let $\lambda(X)$ denote the Lebesgue measure of a measurable set $X \subseteq \mathbb{R}$.

Proposition 4.1. *Fix $c \in \mathbb{R}$. A bounded continuous function $u\colon \mathbb{R} \to \mathbb{R}$ is a traveling wave of (1) with wave speed c if and only if the following holds:*

(TW1) The open set $\mathbb{R}\setminus u^{-1}(N_g)$ is a countable disjoint union $\bigcup_j I_j$ of open intervals I_j. It holds that $u|_{I_j} \in \mathcal{C}^\infty(I_j)$ for all j and $u(s) \notin N_g$ for $s \in \bigcup_j I_j$.

(TW2) There is a $K \in \mathbb{R}$ such that

(a) for each j there exists some $h_j \in \mathbb{R}$ so that u satisfies

$$\begin{cases} (u')^2 = 2\dfrac{h_j-\psi(u)}{\varphi(u)g(u)} & \text{on } I_j \\[2ex] u \to \alpha_i & \text{at finite endpoints of } I_j, \text{ with } \alpha_i \in N_g. \end{cases} \tag{18}$$

(b) If $\lambda(u^{-1}(N_g)) > 0$, then $N_g \cap N_{f_0} \neq \emptyset$, i.e. $K = K_{\alpha_i}(c)$, $i \in \{1,2\}$.[1]

(TW3) u' exists a.e. and $u' \in L^2_{\mathrm{loc}}(\mathbb{R})$.

Remark 4.2. In particular, Proposition 4.1 implies that all traveling wave solutions of (1) can be obtained via a systematic phase plane analysis of (8) for all parameter pairings (c, K).

We give the proof of Proposition 4.1 at the end of this section after stating some auxiliary results.

Lemma 4.3. *Let u be a traveling wave solution of (1) and let $I \subseteq \mathbb{R}$ be an open interval. If the restriction of u on I is $\mathcal{C}^2$, then u solves (5) pointwise on I.*

Proof. The restriction $u|_I$ satisfies (5) in $\mathcal{D}'(I)$, i.e.

$$\int_I [u''g(u) - f(u,u')]\phi\,\mathrm{d}s = 0 \qquad \text{for all} \quad \phi \in \mathcal{D}(I). \tag{19}$$

Now $\rho := u''g(u) - f(u,u')$ is continuous in I by assumption. It follows that ρ is identically zero in I, proving that (5) is satisfied pointwise in I. Indeed, otherwise there would be some $s_0 \in I$ with $\rho(s_0) \neq 0$, say $\rho(s_0) > 0$. By continuity, $\rho > 0$ on a small subinterval I_ε containing s_0. Choosing a nonnegative bump-function $\phi_0 \in \mathcal{D}(I)$ with $\operatorname{supp}(\phi_0) \subseteq I_\varepsilon$ would imply a strictly positive integral in (19) – a contradiction. □

[1] See (29) for the definition of K_{α_i}.

Remark 4.4. Lemma 4.3 tells us in particular that our definition of traveling wave solutions, which is based on a weak formulation of (5) is a consistent generalization of the concept of classical solutions.

Lemma 4.5. *Let u be a traveling wave solution of (1). Then $g^k(u) := (g(u))^k \in \mathcal{C}^2(\mathbb{R})$ for $k \geq 5$.*

Proof. Throughout this proof we consider derivatives $(\cdot)'$, $(\cdot)''$, etc. as distributional derivatives, and terms which contain such derivatives as elements in $\mathcal{D}'$. Once we realize that such distributions actually lie in better spaces, e.g. $W^{1,1}_{\mathrm{loc}}$, the symbol $(\cdot)'$ may be interpreted as a classical (pointwise or pointwise a.e.) derivative.

Note first, that $u''g(u) \in L^1_{\mathrm{loc}}$ because $u''g(u) = f(u,u')$ in $\mathcal{D}'$ by (5) and $f(u,u')$ is a regular distribution (i.e. an element of L^1_{loc}) since $u \in H^1_{\mathrm{loc}}$ by assumption. Therefore, we obtain that $u'g(u) \in W^{1,1}_{\mathrm{loc}}$ since $u'g(u) \in L^1_{\mathrm{loc}}$ and

$$[u'g(u)]' = u''g(u) + (u')^2 g'(u) \in L^1_{\mathrm{loc}}. \tag{20}$$

Similarly, we get that $(u'g(u))^2 \in W^{1,1}_{\mathrm{loc}}$, since $(u')^2 g^2(u) \in L^1_{\mathrm{loc}}$ and

$$[(u'g(u))^2]' = 2u'g(u)[u''g(u) + (u')^2 g'(u)] \in L^1_{\mathrm{loc}}.$$

As a consequence we also have that $u''g^3(u) \in W^{1,1}_{\mathrm{loc}}$, since

$$u''g^3(u) = f(u,u')g^2(u) = f(u,0)g^2(u) + (u')^2 g^2(u)(Gu - B/2),$$

and $(u')^2 g^2(u) \in W^{1,1}_{\mathrm{loc}}$. For $k \geq 4$ we calculate

$$[g^k(u)]' = kg^{k-1}(u)g'(u)u' = kg^{k-4}(u)g'(u)u'g^3(u).$$

Hence, we may write $[g^k(u)]''$ for $k \geq 5$ as

$$\begin{aligned} &k(k-4)g^{k-5}(u)g(u)^2(u')^2 g^3(u) \\ &\quad + kg^{k-4}(u)\Big[g''(u)(u')^2 g^3(u) + g'(u)\Big(u''g^3(u) + 3(u')^2 g^2(u)g(u)\Big)\Big], \end{aligned}$$

which lies in $W^{1,1}_{\mathrm{loc}}$ by our previous considerations. Thus $[g^k(u)]''$ is absolutely continuous and therefore $g^k(u) \in \mathcal{C}^2(\mathbb{R})$ for $k \geq 5$. □

Let us denote by ∂X the set of all boundary points of a subset $X \subseteq \mathbb{R}$, and recall that $N_g = g^{-1}(0)$ defined in (9) is the preimage of 0 under g.

Lemma 4.6. *Let u be a traveling wave solution of (1). Then $u \in C^\infty(\mathbb{R} \setminus \partial(u^{-1}(N_g)))$.*

Proof. The set N_g is either empty, a singleton, or it contains two elements. Assuming that s_0 is an interior point of $u^{-1}(N_g)$, there exists an open interval $I_\varepsilon = (s_0 - \varepsilon, s_0 + \varepsilon) \subseteq u^{-1}(N_g)$. Since u is continuous, $u(I_\varepsilon)$ is a singleton by the mean value theorem. Therefore, the restriction $u|_{I_\varepsilon}$ is a constant function, in other words $u|_{I_\varepsilon} \in \mathcal{C}^\infty(I_\varepsilon)$.

For the remaining part of the proof let $O := \mathbb{R} \setminus u^{-1}(N_g)$. The preimage of the closed set N_g under u is a closed set since u is continuous, and hence O is an open subset. Assuming that $s_0 \in O$, we will find a small open interval I containing s_0, such that the restriction $u|_I \colon I \to \mathbb{R}$ lies in $\mathcal{C}^\infty(I)$, which establishes the claim. For this purpose, let us first denote by $I_\varepsilon := (s_0 - \varepsilon, s_0 + \varepsilon) \subseteq O$ a suitable ε-neighborhood of s_0. The key observation is that $u|_{I_\varepsilon} \in C^2(I_\varepsilon)$. Indeed, by Lemma 4.5 we find that $(g(u))^k$ is $C^2(\mathbb{R})$ for any $k \geq 5$, and hence $g(u)$ is $C^2(\mathbb{R} \setminus u^{-1}(N_g))$. Therefore the restriction of u on I_ε is twice continuously differentiable, since $u(I_\varepsilon) \cap N_g = \emptyset$ by construction. In particular, u has a classical derivative in s_0, say $u'(s_0) =: v_0$;

furthermore we set $u_0 \coloneqq u(s_0)$. Let us consider the following initial value problem on I_ε:

$$\begin{cases} u' = v \\ v' = \dfrac{f(u,v)}{g(u)}, \end{cases} \qquad (u(s_0), v(s_0)) = (u_0, v_0). \tag{21}$$

The classical Picard-Lindelöf theory provides a unique smooth solution $(\bar{u}, \bar{v})$ of (21), at least on a small open subinterval $I \subseteq I_\varepsilon$ with $s_0 \in I$, since the right hand side of (21) is smooth on I_ε. Since $\bar{u} = u|_I$ we conclude that $u|_I \in \mathcal{C}^\infty(I)$, due to our construction and Lemma 4.3. □

Remark 4.7. Lemma 4.6 implies in particular that a traveling wave of (1) with wave speed $c > \bar{c}$ is smooth. An alternative straight forward (but tedious) way to prove Lemma 4.6 is to show that for any given $k \in \mathbb{N}$ one can find some $n \in \mathbb{N}$ such that $g^n(u) \in \mathcal{C}^k(\mathbb{R})$, similarly as in [31].

Lemma 4.8. *Let $w\colon \mathbb{R} \to \mathbb{R}$ be an absolutely continuous function and let $\mathrm{A} \subseteq \mathbb{R}$ be a finite subset. Then the classical derivative w' exists a.e. on $\mathbb{R}$ and $w' = 0$ a.e. on the preimage $w^{-1}(\mathrm{A})$.*

Proof. Let us first prove the special case where A contains only one element, say $\mathrm{A} = \{\alpha\}$, for $\alpha \in \mathbb{R}$. Since w is absolutely continuous, w' exists almost everywhere in $\mathbb{R}$. By continuity, $R \coloneqq w^{-1}(\alpha)$ is a closed subset of $\mathbb{R}$. As a closed set, R is the disjoint union of a perfect set P (i.e. closed without isolated points) and a countable set S, due to the Cantor-Bendixson theorem (see for example [24]). Let $p \in P$ be a point, such that $w'(p)$ exists. We choose a sequence $(p_i)_i$ of points $p_i \in P$ with $p_i \to p$ for $i \to \infty$ in order to see that

$$w'(p) = \lim_{i\to\infty} \frac{w(p) - w(p_i)}{p - p_i} = \lim_{i\to\infty} \frac{\alpha - \alpha}{p - p_i} = 0. \tag{22}$$

Since S is countable, its Lebesgue measure is zero and hence $w' = 0$ a.e. on R.

For the case of a general finite subset A, we apply the same line of arguments as before. We see that the sequence $(w(p_i))_i$ might not be constant but take different values of the finite set A. By the continuity of w however, we infer that $w(p_i) \to w(p)$ as $p_i \to p$. Therefore, the sequence $(w(p_i))_i$ takes the constant value $w(p)$ for almost all $n \in \mathbb{N}$, which shows that the limit in (22) is zero also in the general case. □

Proof of Proposition 4.1. Let us first assume that u is a traveling wave of (1). Thus, $u \in H^1_{\mathrm{loc}}$, hence (TW3) is satisfied. Property (TW1) follows from Lemma 4.6 and its proof, and the fact that every open subset of $\mathbb{R}$ can be represented as a countable union of open intervals. Property (TW2) follows from the fact that u is smooth on I_j and solves the planar differential system (8) on I_j. In Section 3 we proved that this system is integrable and (16) implies the first relation in (18) for some $h_j \in \mathbb{R}$. The continuity of u and (TW1) yield the second assertion in (18). Suppose that $\lambda(u^{-1}(N_g)) > 0$. Since both u and $u'g(u)$ are absolutely continuous in view of the proof of Lemma 4.5, we deduce from Lemma 4.8 that both

$$u' = 0 \quad \text{and} \quad [u'g(u)]' = 0 \quad \text{a.e. on } u^{-1}(N_g), \tag{23}$$

since $u^{-1}(N_g) \subseteq [u'g(u)]^{-1}(\{0\})$. Thus in particular, $u''g(u) = 0$ a.e. on $u^{-1}(N_g)$. In summary this implies, using (5), that $f(u,0) = 0$ on $u^{-1}(N_g)$. Therefore, $K = K_{\alpha_i}$ with $\alpha_i \in N_g$ as defined in (29).

Let us now assume that a bounded continuous function $u\colon \mathbb{R} \to \mathbb{R}$ satisfies (TW1)–(TW3). If $\lambda(u^{-1}(N_g)) = 0$, then u satisfies (5) pointwise a.e. in $\mathbb{R}$ by (TW1) and (TW2). To see this, one has to differentiate the equation in (18) with respect to s, and use the formula (12) for the integrating factor and the fact that u' is nonzero a.e. Due to (TW3) and the boundedness of u, we obtain that $f(u, u')$ is locally integrable. Therefore $u''g(u)$ lies in $L^1_{\mathrm{loc}}(\mathbb{R})$ as well, and since they agree almost everywhere, we obtain:

$$\int_{\mathbb{R}} u''g(u)\,\phi\,\mathrm{d}s = \int_{\mathbb{R}} f(u,u')\,\phi\,\mathrm{d}s \quad \text{for all} \quad \phi \in \mathcal{D}(\mathbb{R}),$$

which means that u is a traveling wave of (1), since we can rewrite this equation in the form (7). For the case $\lambda(u^{-1}(N_g)) > 0$, let us first observe, that $u'g(u) \in W^{1,1}_{\mathrm{loc}}(\mathbb{R})$ and is therefore absolutely continuous. To see this, note that similar to the proof of Lemma 4.5 we obtain

$$u'g(u) \in L^1_{\mathrm{loc}}(\mathbb{R} \setminus u^{-1}(N_g))$$

and

$$[u'g(u)]' = u''g(u) + g'(u)(u')^2 \in L^1_{\mathrm{loc}}(\mathbb{R} \setminus u^{-1}(N_g)),$$

since u is bounded, and both $(u')^2$ and $u''g(u)$ are locally integrable. Therefore (23) holds true and hence $u''g(u) = 0$ a.e. on $u^{-1}(N_g)$. Since $K = K_{\alpha_i}$ with $\alpha_i \in N_g$ and in view of (23), we find that $f(u, u') = 0$ a.e. on $u^{-1}(N_g)$, and therefore equation (5) holds a.e. on $u^{-1}(N_g)$. Since we already know that the equation holds on $\mathbb{R}\setminus u^{-1}(N_g)$ in view of (TW1) and (TW2), we conclude that (5) holds a.e. on $\mathbb{R}$. By (TW3) we obtain that $f(u, u') \in L^1_{\mathrm{loc}}(\mathbb{R})$ and therefore u is a traveling wave solution of (1) in the sense of Definition 2.1. □

5. Construction of traveling wave solutions.

In the current section we construct traveling waves of (1) by combining solution curves of (8) in a suitable way. According to Proposition 4.1 we can obtain all traveling waves of (1) by following this approach. For the study of these solution curves we exploit the fact that (8), and the topologically equivalent system (11), are integrable on U and the respective solution curves are the level sets $L_h(H)$ of the first integral H, which can be expressed in the form (16). In particular, we observe that the functions f_0, g and φ fully determine the phase portrait of the systems (8) and (11) for a given pair $(c, K) \in \mathbb{R}^2$.

Before studying the qualitative behavior of the solution curves in detail, we give a rough overview of the phase portraits of (11) by discussing the fixed points for all parameter combinations (c, K). After that, we provide explicit formulae for the integrating factors φ for all wave speeds c and summarize their basic properties.

5.1. Fixed points of system (11).

The fixed points of system (11) are of the form $(u, 0)$ and (α_i, v), where $\alpha_i \in N_g$, $i \in \{1, 2\}$, denote the real zeros of g, cf. (9). The number and type of fixed points are determined by the zeros of the polynomials g and f_0, which vary with the parameters c and K.

Fixed points of the form $(u, 0)$ on the horizontal axis are determined by the roots of $f_0(u) = f(u, 0)$. For any wave speed $c \in \mathbb{R}$, we denote by $K_0 = K_0(c)$ the zero of the discriminant $\Delta_{f_0} := (c-1)^2 - 4EK$ of the quadratic polynomial f_0, that is,

$$K_0 := \frac{(c-1)^2}{4E}. \tag{24}$$

Then f_0 has a double root $\bar{u}$ when $K = K_0$, it has two zeros $u_1 < \bar{u} < u_2$ whenever $K > K_0$, where

$$u_i = \frac{1 - c \pm \sqrt{\Delta_{f_0}}}{2E}, \ i = 1, 2,$$

and $f_0 < 0$ if $K < K_0$. Provided that N_g is nonempty, there exist invariant vertical lines $\{u = \alpha_i\}$, where $\alpha_i \in N_g, i = 1, 2$. These invariant sets exist for wave speeds $c \leq \bar{c}$, where

$$\bar{c} := \frac{64}{105} \tag{25}$$

is the zero of the discriminant $\Delta_g = B^2 - 4A_cC$ of the quadratic polynomial g. Then g is strictly positive if and only if $c > \bar{c}$ and $g(u) = C(u - \alpha_1)(u - \alpha_2)$ if $c \leq \bar{c}$, with

$$\alpha_i = \frac{-B \pm \sqrt{\Delta_g}}{2A_c}, \ i = 1, 2. \tag{26}$$

Note that the two zeros of g coincide precisely when $c = \bar{c}$ in which case we denote the double root of $g(u)$ by α. Observe that $\bar{u}(c) < \alpha_1(c) < \alpha_2(c)$ for all $c \in (-\infty, \bar{c})$ and $\bar{u}(\bar{c}) < \alpha$ as displayed in Fig. 2a. The second component of the fixed point (α_i, v) is determined by the relation $f(\alpha_i, v) = 0$, which we will analyze below.

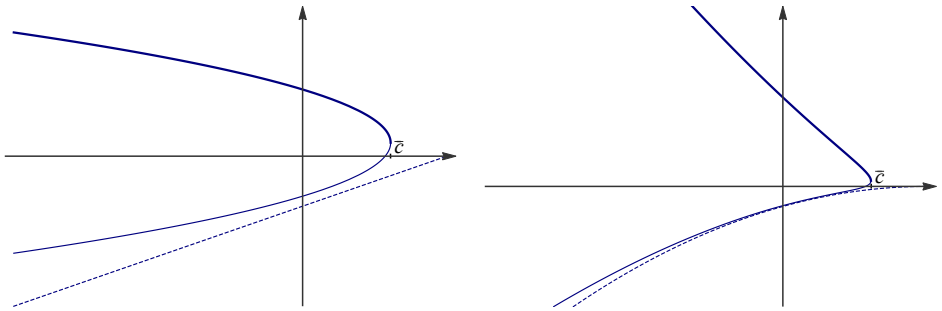

(a) (b)

FIGURE 2. (a) the graphs of the functions α_2 [bold], α_1 [plain] and $\bar{u}$ [dashed]; (b) the graphs of K_{α_2} [bold], K_{α_1} [plain] and K_0 [dashed], cf. (24) and (29).

Next we determine the type of fixed points $(u, 0)$. The Jacobian of a point $(u, v) \in \mathbb{R}^2$ of (11) is given by

$$J(u, v) = \begin{pmatrix} vg'(u) & g(u) \\ \partial_u f(u, v) & \partial_v f(u, v) \end{pmatrix}. \tag{27}$$

We recall that system (11) is integrable on $U = \mathbb{R}^2 \setminus (N_g \times \mathbb{R})$. Therefore, the type of any fixed point in U is determined by the sign of the determinant of the Jacobian at the fixed point: a negative determinant implies a saddle, a positive determinant implies a center and a vanishing determinant implies a cusp. The determinant of J at the fixed points $(u_i, 0) \in U$ is given by

$$\det[J(u_i, 0)] = \mp\sqrt{\Delta_{f_0}}\, g(u_i), \quad i = 1, 2. \tag{28}$$

Therefore, its sign depends on the positions of the fixed points $(u_i, 0)$ relative to each other and the invariant lines $\{u = \alpha_i\}, i = 1, 2$. Whenever these invariant lines

exist, that is, for $c \leq \bar{c}$, we define the values $K_{\alpha_i}(c)$ as follows:

$$K_{\alpha_i}(c) \text{ denotes the unique zero of } u_2(c,K) - \alpha_i(c),\ i = 1,2. \tag{29}$$

That is, for each $c \leq \bar{c}$ the root α_i of $g(u)$ coincides with the root u_2 of $f_0(u)$ precisely when $K = K_{\alpha_i}(c)$. The relative positions of $u_1(c,K)$, $u_2(c,K)$, $\alpha_1(c)$ and $\alpha_2(c)$, and hence the sign of (28), are determined by the relative position of K with respect to $K_0(c)$, $K_{\alpha_1}(c)$ and $K_{\alpha_2}(c)$, cf. Fig. 2b. Since $K_0(c) < K_{\alpha_1}(c) < K_{\alpha_2}(c)$ for all $c \in (-\infty, \bar{c})$, and $K_0(\bar{c}) < K_\alpha$, there are precisely seven different scenarios which classify the types of fixed points lying on the u-axis. We summarize them in Table 1.

scenario	parameter	order relation	fixed points and type
I	$K < K_0(c)$	-	-
II	$K = K_0(c)$	$\bar{u} < \alpha_1 < \alpha_2$	$(\bar{u}, 0)$ n
III	$K_0(c) < K < K_{\alpha_1}(c)$	$u_1 < u_2 < \alpha_1 < \alpha_2$	$(u_1, 0)$ s, $(u_2, 0)$ c
IV	$K = K_{\alpha_1}(c)$	$u_1 < u_2 = \alpha_1 < \alpha_2$	$(u_1, 0)$ s, $(\alpha_1, 0)$ n
V	$K_{\alpha_1}(c) < K < K_{\alpha_2}(c)$	$u_1 < \alpha_1 < u_2 < \alpha_2$	$(u_1, 0)$ s, $(u_2, 0)$ s
VI	$K = K_{\alpha_2}(c)$	$u_1 < \alpha_1 < u_2 = \alpha_2$	$(u_1, 0)$ s, $(\alpha_2, 0)$ n
VII	$K > K_{\alpha_2}(c)$	$u_1 < \alpha_1 < \alpha_2 < u_2$	$(u_1, 0)$ s, $(u_2, 0)$ c

TABLE 1. A list of all possible scenarios for the ordering of fixed points on the horizontal axis. Here s stands for saddle, c for center and n means that the Jacobi matrix at the fixed point is nilpotent.

The local behavior near the nilpotent fixed points will be determined in the phase plane analysis in Section 5.4. Let us point out, that in the situation $c = \bar{c}$, i.e. when $g(u)$ has the double root α, we distinguish between the five scenarios I–IV and VII in Table 1, since $K_\alpha(\bar{c}) = K_{\alpha_1}(\bar{c}) = K_{\alpha_2}(\bar{c})$. In case that $c > \bar{c}$, i.e. when N_g is empty, we distinguish only between the first three scenarios, where K has no upper bound in scenario III.

To determine the type of the fixed points (α_i, v), $i \in \{1,2\}$, on the invariant lines, recall that their second component is determined by the relation $f(\alpha_i, v) = 0$, which holds if and only if $v = \pm v_{\alpha_i}$, where

$$v_{\alpha_i} := \sqrt{\frac{-f_0(\alpha_i)}{-\frac{1}{2}B + G\alpha_i}}$$

whenever this expression is real and finite. We observe that

$$-\frac{1}{2}B + G\alpha_2(c) < 0 \quad \text{for all } c \in (-\infty, \bar{c}), \tag{30}$$

thus the fixed points $(\alpha_2, \pm v_{\alpha_2})$ exist whenever $f_0(\alpha_2) > 0$, that is, for $K > K_{\alpha_2}(c)$ defined in (29). These fixed points are saddles, since the local linearization of (11), which is a lower triangular matrix in view of (27), has two nonzero eigenvalues of opposite sign. The existence of the fixed points $(\alpha_1, \pm v_{\alpha_1})$ does not depend solely on K, but also on the parameter c, since $-\frac{1}{2}B + G\alpha_1(c)$ changes its sign at the particular wave speed

$$c_1 := \frac{24505}{41503} < \bar{c}. \tag{31}$$

We find that $\pm v_{\alpha_1}$ are real numbers – and hence the points $(\alpha_1, \pm v_{\alpha_1})$ are fixed points of (11) – provided that either $c < c_1$ and $K < K_{\alpha_1}(c)$ or $c \in (c_1, \bar{c})$ and

$K > K_{\alpha_1}(c)$. In the first case, $(\alpha_1, \pm v_{\alpha_1})$ are saddles since the Jacobian J is a lower triangular matrix with eigenvalues of opposite sign. In the second case, these fixed points are stable or unstable nodes, i.e. both eigenvalues of their lower triangular matrix J are nonzero real numbers of the same sign. In the case that $K = K_{\alpha_1}(c)$ and $c \in (-\infty, \bar{c}) \setminus \{c_1\}$, we have $v_{\alpha_1} = 0$, hence the corresponding fixed point lies on the horizontal axis and the situation is as described in scenario IV in Table 1. Similarly, the case $K = K_{\alpha_2}(c)$, where $v_{\alpha_2} = 0$ for all $c \in (-\infty, \bar{c})$, corresponds to scenario VI. It remains to discuss the case $c = c_1$ and $K = K_{\alpha_1}(c_1)$ for which the function f can be written as

$$f(u, v) = E(u - u_1)(u - \alpha_1(c_1)) - G(u - \alpha_1(c_1))v^2.$$

This implies that every point on the invariant line $\{u = \alpha_1(c_1)\}$ is a fixed point of system (11).

If $c = \bar{c}$, the function g has a unique double root at $u = \alpha$ and for $K > K_\alpha$ we have that the fixed points $(\alpha, \pm v_\alpha)$ are non-hyperbolic.

5.2. **Integrating factor.** In this subsection, we give explicit formulas for the integrating factor φ of system (11) for various wave speeds. Recall that φ solves the differential equation (12). Obviously, its explicit form depends on the number of real roots of the polynomial g, and thus on the wave speed c. Therefore, we treat the three cases $c > \bar{c}$, $c = \bar{c}$ and $c < \bar{c}$ separately.

5.2.1. *Case $c > \bar{c}$.* We have that $g > 0$, hence we may define $\gamma := \sqrt{-\Delta_g} \in \mathbb{R}^+$. We find that the positive real analytic function

$$\varphi(u) = (g(u))^\rho \exp\left(-\frac{2\rho B}{\gamma} \arctan\left(\frac{g'(u)}{\gamma}\right)\right) \tag{32}$$

solves (12) in $\mathbb{R}$, where we have set $\rho := -\left(1 + \frac{G}{C}\right) > 0$, cf. Fig. 3a. The first integral H associated to φ is analytic in $\mathbb{R}^2$.

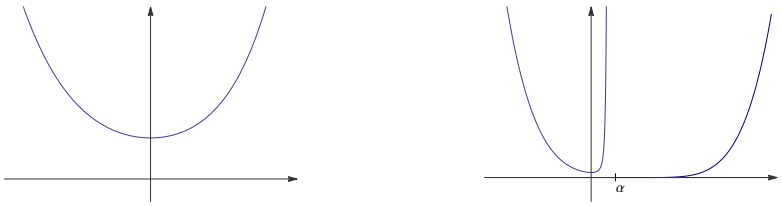

(a) (b)

FIGURE 3. The graph of φ for (a) $c > \bar{c}$ and (b) $c = \bar{c}$.

5.2.2. *Case $c = \bar{c}$.* In this situation, the polynomial g has a double root in α, cf. (26), so that $g(u) = C(u - \alpha)^2$, and

$$\varphi(u) = \left(\frac{g(u)}{C}\right)^\rho \exp\left(-2\rho \frac{\alpha}{u - \alpha}\right) > 0 \tag{33}$$

solves (12) in $\mathbb{R} \setminus \{\alpha\}$, where again $\rho = -\left(1 + \frac{G}{C}\right) > 0$. We note that φ is real analytic and strictly positive in its domain $\mathbb{R} \setminus \{\alpha\}$, cf. Fig. 3b. Therefore, the first integral H associated to φ is analytic in $U = \mathbb{R} \setminus \{\alpha\}$.

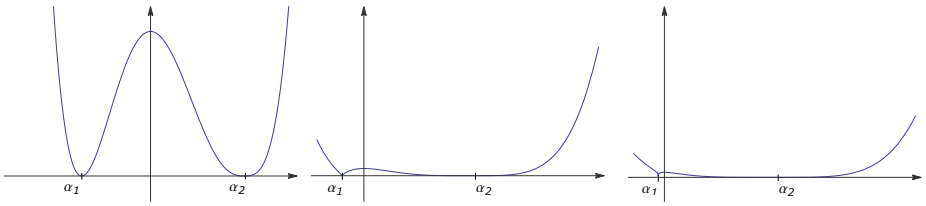

(a) (b) (c)

(a)-(c): $c \in (-\infty, 4/7)$ and φ is continuous with two zeros at $\alpha_{1,2}$.

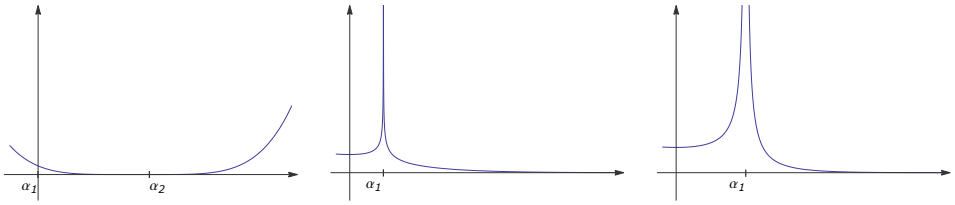

(d) $c = 4/7$: $\varphi^{-1}(0) = \{\alpha_2\}$. (e) $c \in (4/7, c_1)$: $\varphi \in H^1_{\mathrm{loc}}$. (f) $c \in [c_1, \bar{c})$: $\varphi \notin H^1_{\mathrm{loc}}$.

FIGURE 4. The graph of φ for increasing values of $c \in (-\infty, \bar{c})$.

5.2.3. *Case* $c < \bar{c}$. We have that $g(u) = C(u-\alpha_2)(u-\alpha_1)$ and

$$\varphi(u) = \Big(|u-\alpha_2|^{\alpha_2}|u-\alpha_1|^{-\alpha_1}\Big)^{\theta_c} \tag{34}$$

solves (12) in $\mathbb{R} \setminus \{\alpha_1, \alpha_2\}$, where

$$\theta_c := -\frac{2\big(1+\frac{G}{C}\big)}{\alpha_2(c)-\alpha_1(c)} > 0.$$

Note that φ is real analytic and positive in $U = \mathbb{R} \setminus \{\alpha_1, \alpha_2\}$ and $\varphi \in \mathcal{C}(\mathbb{R})$ as long as $\alpha_1 \le 0$, cf. Fig. 4. For all $c < \bar{c}$ we have that $\lim_{|u|\to\infty} \varphi(u) = \infty$ and that φ is continuous in α_2 with $\varphi(\alpha_2) = 0$, while

$$\lim_{u\to\alpha_1} \varphi(u) = \begin{cases} 0 & \text{if} \quad \alpha_1 < 0 \\ (\alpha_2-\alpha_1)^{\theta_c\alpha_2} & \text{if} \quad \alpha_1 = 0 \\ \infty & \text{if} \quad \alpha_1 > 0. \end{cases}$$

Formula (34) tells us that φ has a certain regularity in α_2, and also in α_1 provided that α_1 is small enough. Furthermore we deduce from (34) that $\varphi \in L^1_{\mathrm{loc}}(\mathbb{R})$ if and only if $\alpha_1(c)\theta_c < 1$, which holds true if and only if $c < c_1$. Recall that c_1, defined in (31), is the bifurcation value for the existence of fixed points of the form $(\alpha_1, \pm v_{\alpha_1})$. Moreover, we see that the function $\psi = -\int f_0\varphi\,\mathrm{d}u$ is continuous at α_1 if $c < c_1$. Observe that ψ is continuous even for wave speeds slightly larger then c_1 if α_1 is a root of f_0. More precisely, for $c \in (-\infty, \bar{c})$ we consider $f_0 = f_0(c, K)$ and set $K = K_{\alpha_1(c)}$ so that f_0 vanishes at $u_2(c, K_{\alpha_1}) = \alpha_1(c)$, cf. (29). We define

$$c_2 := \sup\{c \in (-\infty, \bar{c}) : f_0\varphi \in L^1_{\mathrm{loc}}(\mathbb{R})\}, \tag{35}$$

and find that $c_2 = \sup\{c \in (-\infty, \bar{c}) : \alpha_1(c)\,\theta_c < 2\} = \frac{165796}{277207}$. Then $\psi \in \mathcal{C}(\mathbb{R})$ if and only if $c < c_2$. We clearly have that

$$c_1 < c_2 < \bar{c}.$$

This concludes our discussion of the fixed points and integrating factor of system (11). The remainder of this section deals with the systematic construction of traveling wave solutions of (1).

5.3. **Traveling waves – the "smooth" case.** We claim that for any $c > \bar{c}$ and $K > K_0(c)$ there exist smooth solitary and smooth periodic traveling waves. Indeed, recall that when $c > \bar{c}$ we have $g(u) > 0$, and the first integral is of the form (32). Therefore H is analytic on $\mathbb{R}^2$ with $\nabla H(u, v) = 0$ if and only if $v = 0$ and $\psi'(u) = 0$. In view of the fact that $\frac{v^2}{2}\varphi(u)g(u) \geq 0$, we find that $(u_2, 0)$ is a local minimum of H whereas $(u_1, 0)$ is a saddle point since

$$\psi''(u) = -(\varphi(u)f_0(u))' = \varphi(u)\left(f_0(u)\frac{2(C+G)u}{g(u)} - f_0'(u)\right), \tag{36}$$

implying that

$$\psi''(u_1) = -\varphi(u_1)f_0'(u_1) = -\varphi(u_1)\sqrt{\Delta_{f_0}} < 0, \quad \psi''(u_2) = \varphi(u_2)\sqrt{\Delta_{f_0}} > 0,$$

where Δ_{f_0} is the discriminant of f_0 defined in Section 5.1. Note that $H(u, 0) = \psi(u)$ with $\lim_{u\to\pm\infty}\psi(u) = \pm\infty$, and $\lim_{|v|\to\infty} H(u, v) = \infty$, for any fixed $u \in \mathbb{R}$. Since ψ decreases strictly in the interval (u_1, u_2) and increases strictly in (u_2, ∞), there exists precisely one $u_r \in (u_2, \infty)$ with $\psi(u_1) = \psi(u_r)$. Thus, the level-set $L_{h_1}(H)$ contains the two branches $\{(u, v_{h_1}^{\pm}(u))\colon u \in [u_1, u_r]\}$ for $h_1 \coloneqq \psi(u_1)$ and $v_{h_1}^{\pm}(u)$ given in (16), which form a homoclinic orbit of system (8) representing a smooth solitary traveling wave of (1). This solution is symmetric with respect to its unique maximum in view of the symmetry of H in the second variable, cf. (13). Moreover, the solitary wave decays exponentially to the constant value u_1 on either side of the maximum at infinity, since the vector field is locally $\mathcal{C}^1$-conjugate to its linearization at the hyperbolic saddle $(u_1, 0)$ by the Hartman-Grobman Theorem, cf. [37].

The level-sets $L_h(H)$ with $h \in (\psi(u_2), \psi(u_1))$ correspond to periodic orbits around the center $(u_1, 0)$ of system (8), that is, closed loops contained in the region bounded by the homoclinic orbit corresponding to $h = h_1$. These periodic orbits represent smooth periodic traveling wave solutions of (1) which are symmetric with respect to their local extrema and have a unique maximum and minimum per period.

These are all non-constant solutions of (8) for $K > K_0$ which are bounded in the u-component. In Fig. 5 we indicate the unbounded solutions by grey lines. There are no non-trivial bounded solutions for $K \leq K_0$, cf. Table 1. Indeed, for $K < K_0$ the system has no critical points, while for $K = K_0$ it has a nilpotent fixed point (a cusp), hence there are no non-constant orbits in the phase plane, which are bounded in the u-component.

5.4. **Traveling waves – the "singular" case.** We recall that the zero set N_g of the quadratic polynomial g is nonempty for wave speeds $c \leq \bar{c}$. This yields the existence of one invariant vertical line $\{u = \alpha\}$ in the phase plane of (11) if $c = \bar{c}$ and $N_g = \{\alpha\}$, or two such lines $\{u = \alpha_1\}$ and $\{u = \alpha_2\}$ if $c < \bar{c}$ and $N_g = \{\alpha_1, \alpha_2\}$. These lines form the complement of the domain $U \subseteq \mathbb{R}^2$ of system (8). However, it turns out that for certain parameter combinations $(c, K) \in (-\infty, \bar{c}] \times \mathbb{R}$ solutions of (8) can have a continuous extension to a fixed point of (11) of the form $(\alpha_i, \pm v_{\alpha_i})$, $i \in \{1, 2\}$, on $N_g \times \mathbb{R}$, and possible even beyond that point. It may also happen that a solution of (8) becomes unbounded in its v-component as its u-component approaches an element of N_g. In view of Proposition 4.1 we will combine such solutions of system (8), which are defined not globally, but on subintervals of $\mathbb{R}$, in

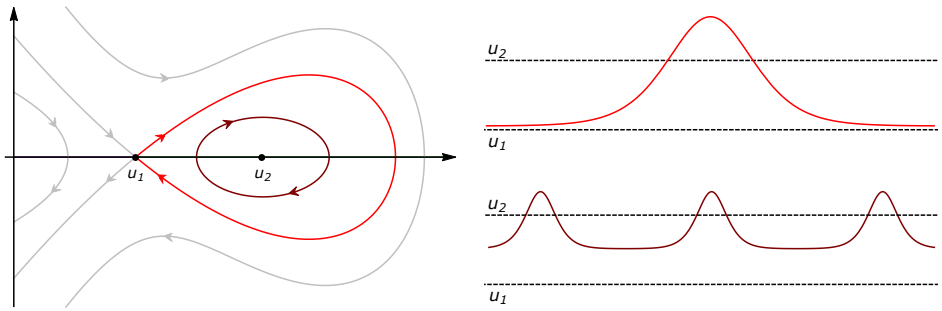

(a) (b)

FIGURE 5. In (5a) we sketch a phase portrait representing scenario III in Table 1, which yields a smooth solitary and smooth periodic traveling waves as illustrated in (5b).

a suitable way to construct non-smooth traveling waves of (1). In Example 5.3 we explain a prototypical construction in full detail.

We discuss the cases $c < \bar{c}$ in Section 5.4.1 and the case $c = \bar{c}$ in Section 5.4.2. For each scenario we provide sketches of the corresponding phase portraits. Let us point out that the orientation of the orbits – indicated by arrows – reflects the parametrization of system (8). For convenience, also fixed points of the form (α_i, v), $i = 1, 2$, of the reparametrized system (11) are included in the sketches, even though they are not contained in the domain U of (8).

5.4.1. *Case* $-\infty < c < \bar{c}$. For this parameter range our qualitative analysis distinguishes between the scenarios I–VII of Table 1. Moreover, we divide each scenario into the subcases $c < c_1$, $c = c_1$ and $c_1 < c < \bar{c}$, where c_1 defined in (31) is the bifurcation value for fixed points on the invariant line $\{u = \alpha_1\}$. It is convenient to consider the following c-dependent subregions of the (u, v)-plane

$$L := \{(u, v) \in \mathbb{R}^2 \colon -\infty < u < \alpha_1\}$$
$$M := \{(u, v) \in \mathbb{R}^2 \colon \alpha_1 < u < \alpha_2\}$$
$$R := \{(u, v) \in \mathbb{R}^2 \colon \alpha_2 < u < \infty\}.$$

Furthermore we denote by L^+, M^+, and R^+ the intersection of L, M and R respectively with the upper half-plane $\mathbb{R} \times \mathbb{R}^+$. We define the lower half-regions L^-, M^- and R^- accordingly. In the following we will refer to the restrictions of level sets $L_h(H)$ to these regions as segments. We will often analyze the regions L, M and R separately. Let us emphasize, however, that orbits may cross the invariant lines through fixed points.

In the constructions below we will frequently discover solution curves of (8) that give rise to global piecewise defined continuous functions $\hat{u} : \mathbb{R} \to \mathbb{R}$ satisfying properties (TW1) and (TW2) of Proposition 4.1. If all involved orbits are not only bounded in the u-component but also in the v-component, then property (TW3) of Proposition 4.1, which ensures that $\hat{u} \in H^1_{\mathrm{loc}}(\mathbb{R})$, is trivially satisfied as well and hence $\hat{u}$ turns out to be a traveling wave solution of (1). The following result clarifies under which conditions property (TW3) is still satisfied in the case that certain involved orbits become unbounded in the v-component.

Lemma 5.1. *Let $(c,K) \in (-\infty,\bar{c}) \times \mathbb{R}$, let $h \in \mathbb{R}$ and suppose that α_i, $i \in \{1,2\}$, is an adherent point of the u-component of the level set $L_h(H) \subseteq U$. Let $\omega = (\omega_1,\omega_2) : I \to U$ be a maximal solution of (8), whose orbit is contained in $L_h(H) = \{(u, v_h^{\pm}(u))\}$.*

(i) If $\lim_{u\to\alpha_2} v_h^+(u) = \infty$, then ω is not suitable for the construction of a traveling wave solution of (1).

(ii) Suppose that assumption (i) is not satisfied. If $\lim_{u\to\alpha_1} v_h^+(u) = \infty$, then ω is suitable for the construction of a traveling wave solution of (1), if and only if ω_1 is bounded and $c \in (c_0, c_1]$, where

$$c_0 := 511/1024. \tag{37}$$

Proof. First we observe the following. If v_h^+ blows up as $u \to \alpha_i$, $i \in \{1,2\}$, then the blow up of ω_2 happens on a finite subinterval of I. To this end, we assume without loss of generality that ω runs through the set $\{(u, v^+(u))\colon \alpha_i - \varepsilon \le u < \alpha_i\}$, $i \in \{1,2\}$, where $\varepsilon > 0$ is sufficiently small, and $\lim_{u\nearrow\alpha_i} v_h^+(u) = \infty$. In view of (17) we see that ω passes this set within a finite interval of length

$$\delta(\varepsilon) = \int_{\alpha_i-\varepsilon}^{\alpha_i} \frac{\mathrm{d}u}{v_h^+(u)} < \infty. \tag{38}$$

More precisely we have that $\delta(\varepsilon) = |s_1 - s_\varepsilon|$, where s_ε is defined via $\omega(s_\varepsilon) = (\alpha_i - \varepsilon, v_h^+(\alpha_i - \varepsilon))$, and $s_1 \in \mathbb{R}$ is the boundary point of the interval I where the blow up of ω occurs, that is,

$$\lim_{s\to s_1} \omega_1(s) = \alpha_i \quad \text{and} \quad \lim_{s\to s_1} \omega_2(s) = \infty.$$

Ad (i). We show that $\omega_2 \notin L^2_{\mathrm{loc}}(I)$. Let us assume that $\{(u, v_h^+(u))\colon \alpha_2 - \varepsilon \le u < \alpha_2\} = \omega([s_\varepsilon, s_1))$ for some $\varepsilon > 0$ sufficiently small with $\lim_{u\nearrow\alpha_2} v_h^+(u) = \infty$ such that $\omega(s_\varepsilon) = (\alpha_2 - \varepsilon, v_h^+(\alpha_2 - \varepsilon))$ with $\lim_{s\to s_1} \omega_1(s) = \alpha_2$ and $\lim_{s\to s_1} \omega_2(s) = \infty$. Observe that $h \neq \psi(\alpha_2)$, since otherwise this limit would be zero in the case $K = K_{\alpha_2}$ and equal to v_{α_2} in case that $K > K_{\alpha_2}$, as an application of de l'Hôpital's rule shows:

$$\begin{aligned}\lim_{u\to\alpha_2} (v_h^+(u))^2 &= \lim_{u\to\alpha_2} 2\frac{h-\psi(u)}{\varphi(u)g(u)} = \lim_{u\to\alpha_2} \frac{-2\psi'(u)}{g'(u)\varphi(u) + g(u)\varphi'(u)} \\ &= \lim_{u\to\alpha_2} \frac{2f_0(u)\varphi(u)}{\varphi(u)[g'(u) - 2(G+C)u]} = \frac{f_0(\alpha_2)}{\frac{1}{2}B - G\alpha_2},\end{aligned}$$

where $\frac{1}{2}B - G\alpha_2 > 0$ for all $c \in (-\infty,\bar{c})$, as discussed in (30). Since ψ is continuous on (α_1,∞), we infer that $h - \psi$ is bounded on $[\alpha_2 - \varepsilon, \alpha_2]$ and for sufficiently small $\varepsilon > 0$ we may assume that $|h - \psi| > \delta$ on $[\alpha_2 - \varepsilon, \alpha_2]$ for some $\delta > 0$. Therefore we obtain that

$$v_h^+(u) = \sqrt{2\frac{h-\psi(u)}{g(u)\varphi(u)}} \in \Theta(|u-\alpha_2|^{-(1+\theta_c\alpha_2)/2}) \quad \text{for} \quad u \nearrow \alpha_2,$$

where

$$\frac{1+\theta_c\alpha_2}{2} \ge 1 \quad \text{for all} \quad c \in (-\infty,\bar{c}). \tag{39}$$

From (17) we obtain that

$$\int_{s_\varepsilon}^{s_1} [\omega_2(s)]^2\,\mathrm{d}s = \int_{\alpha_2-\varepsilon}^{\alpha_2} v_h^+(u)\,\mathrm{d}u, \tag{40}$$

hence ω_2 is not locally square integrable by (39).

Ad (ii). For $c < c_1$ we use the analogous notation and simplifying assumptions as in the proof of part (i). In this case we obtain by similar arguments as in the proof of part (i) that

$$v_h^+(u) \in \Theta(|u-\alpha_1|^{-(1-\theta_c\alpha_1)/2}) \quad \text{for} \quad u \nearrow \alpha_1. \tag{41}$$

Therefore, the corresponding integral in (40) is convergent, and hence $\omega_2 \in L^2_{\mathrm{loc}}(I)$, if and only if

$$\frac{1-\theta_c\alpha_1}{2} < 1, \tag{42}$$

which is equivalent to requiring that $c > c_0$. For the case $c = c_1$, we recall that ψ develops a singularity in α_1, provided that $K \neq K_{\alpha_1}(c_1)$ (if $K = K_{\alpha_1}(c_1)$, we use the same reasoning as above). However, since $g\varphi \in \Theta(1)$ for $u \nearrow \alpha_1$ and $\sqrt{|h-\psi|} \in L^1_{\mathrm{loc}}(\mathbb{R})$, we infer that the corresponding integral (40) is finite also in this case. □

Remark 5.2. We point out that Lemma 5.1 does not tell us whether there exist solutions as stated in the assumptions. We will see that there exist no solutions of (11) which become unbounded in the second component at α_1 if $c > c_1$. Note that $c_0 < c_1$.

In order to get a first impression of the construction of non-smooth traveling waves of (1), we provide a very detailed description of the construction of one particular wave in the following example.

Example 5.3 (A cusped solitary wave)**.** Let $K \in (K_{\alpha_1}(c), K_{\alpha_2}(c))$, i.e. we find ourselves in scenario V of Table 1, and let $c \in (-\infty, c_1)$. The corresponding phase portrait is sketched in Fig. 12a. The function $\psi\colon \mathbb{R} \to \mathbb{R}$ is continuous, and it is smooth on $\mathbb{R} \setminus \{\alpha_1, \alpha_2\}$. We restrict our attention to the region L and observe that ψ increases strictly on $(-\infty, u_1)$, takes a local maximum in u_1 – recall that $(u_1, 0)$ is a saddle – and decreases strictly on (u_1, α_1). Let $h := \psi(u_1)$ and consider the two branches $\{(u, v_h^{\pm}(u))\colon u_1 < u < \alpha_1\}$. The corresponding orbits are indicated by red lines emerging from the saddle point in Fig. 12a: v_h^+ increases strictly on (u_1, α_1) and becomes unbounded as $u \nearrow \alpha_1$, as an application of de L'Hôpital shows. We use these two branches to construct a solitary cusped traveling wave. To this end, recall that s is the moving frame variable corresponding to the wave speed c, that is, s is the independent variable of system (8). We choose $s_0 \in (-\infty, 0)$, let $(u_0, v_0) \in \{(u, v_h^+(u))\colon u_1 < u < \alpha_1\}$ be a point on the upper branch, and consider the Cauchy problem of (8) with initial condition $(u(s_0), v(s_0)) = (u_0, v_0)$. The solution, denoted by $\omega^- = (\omega_1^-, \omega_2^-)$, runs through the upper branch by construction. It is clear that the maximal interval of existence I^- is of the form $(-\infty, s^*)$ with $s^* \in (s_0, \infty)$. Indeed, $\omega^-(s)$ approaches the saddle $(u_1, 0)$ for $s \to -\infty$, and the upper bound is obtained from (17), since

$$s_1 - s_0 = \int_{u_0}^{\alpha_1} \frac{\mathrm{d}u}{v_h^+(u)} < \infty,$$

for a unique finite $s_1 \in \mathbb{R}$. Let us for simplicity assume that $s^* = 0$, i.e. $I^- = (-\infty, 0)$, then

$$\lim_{s\to-\infty}(\omega_1^-(s), \omega_2^-(s)) = (u_1, 0), \quad \lim_{s\nearrow 0}\omega_1^-(s) = \alpha_1, \quad \lim_{s\nearrow 0}\omega_2^-(s) = \infty.$$

Similarly we obtain a solution ω^+ of (8) satisfying $(\omega_1^+(s_0), \omega_2^+(s_0)) = (u_0, -v_0)$, which is defined on $I^+ = (0, \infty)$ and runs through the lower branch with

$$\lim_{s\to\infty} (\omega_1^+(s), \omega_2^+(s)) = (u_1, 0), \quad \lim_{s\searrow 0} \omega_1^+(s) = \alpha_1, \quad \lim_{s\searrow 0} \omega_2^+(s) = -\infty.$$

We are now ready to construct a composition of these wave segments by defining the bounded continuous function $\hat{u}\colon \mathbb{R} \to \mathbb{R}$ as

$$\hat{u}(s) := \begin{cases} \omega_1^- & \text{for} \quad s \in I^- \\ \alpha_1 & \text{for} \quad s = 0 \\ \omega_1^+ & \text{for} \quad s \in I^+, \end{cases}$$

which is smooth on $\mathbb{R} \setminus \{0\}$ and decreases exponentially to u_1 for $|s| \to \infty$, cf. the upper sketch in Fig. 9b. Due to our construction, $\hat{u}$ clearly satisfies properties (TW1) and (TW2) of Proposition 4.1, independent of the value $c \in (-\infty, c_1)$. It remains to confirm (TW3), i.e. to show that the weak derivative $\hat{u}'$ lies in $L^2_{\mathrm{loc}}(\mathbb{R})$, in order to infer that $\hat{u}$ is indeed a traveling wave of (1). In view of Lemma (5.1) we find that $\hat{u}' \in L^2_{\mathrm{loc}}(\mathbb{R})$ if and only if $c > c_0$, with c_0 defined in (37).

A similar construction yields cusped periodic traveling waves, cf. the lower sketch in Fig. 9b. Indeed, for $c \in (c_0, c_1)$ and $K \in (K_{\alpha_1}(c), K_{\alpha_1}(c))$, each $h \in (\psi(\alpha_1), \psi(u_1))$ corresponds to an orbit similar to the one indicated by the wine red line in Fig. 12a. We identify such an orbit with a smooth solution of (8) on some bounded open interval, which may be continued periodically and continuously on the whole real line. Since $c > c_0$, the weak derivative of this function is locally square integrable, and hence this periodic extension clearly satisfies all properties of Proposition 4.1.

In the sequel we will omit the details of such "gluing-processes" in our constructions and just identify suitable combinations of orbits in the phase plane of (8) with traveling waves of (1).

Remark 5.4. In the sketches of the phase portraits for scenarios I–IIV we display orbits which are bounded in the u-component and satisfy Lemma 4.1 (i) with dashed lines to indicate that they are not suitable to construct traveling waves of (1).

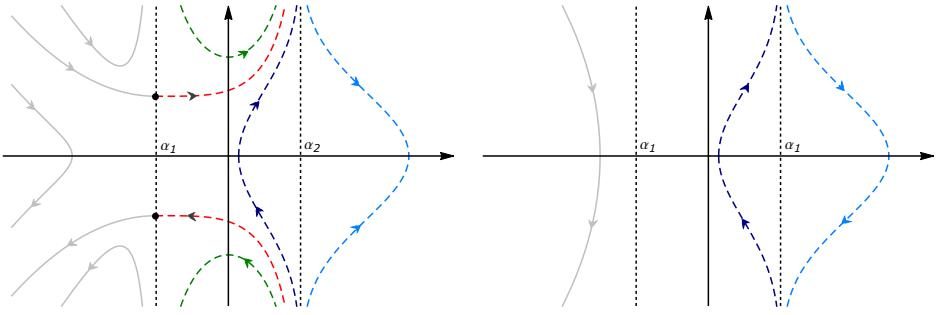

(a) $c < c_1$ (b) $c \in [c_1, \bar{c})$

FIGURE 6. Sketches of phase portraits for scenario I, i.e. $K < K_0(c)$.

Scenario I [Fig. 6]. We begin with the case $c < c_1$, cf. Fig. 6a, where system (11) has two saddles $(\alpha_1, \pm v_{\alpha_1})$ and no other fixed points. The continuous function $\psi\colon \mathbb{R} \to \mathbb{R}$ is strictly increasing.

The orbits in L^+ can be grouped into the following three categories: orbits corresponding to the segment $\{(u, v_h^+(u)) \colon -\infty < u < \alpha_1\}$ for the level $h = \psi(\alpha_1)$, which reach the fixed point (α_1, v_{α_1}) and separate L^+ into an upper region with orbits of the form $\{(u, v_h^+(u)) \colon -\infty < u < \alpha_1\}$ for the levels $h > \psi(\alpha_1)$, and a lower region with orbits corresponding to the level sets $\{(u, v_h^+(u)) \colon -\infty < u < r\}$ for $h < \psi(\alpha_1)$, $r < \alpha_1$, with $\lim_{u \to -\infty} v_h^+ = \infty$ in each case. By the symmetry of the system we obtain the analogous picture for L^-. We sketch these orbits with gray lines in Fig. 6a since they are unbounded in the first component and therefore do not give rise to traveling wave solutions.

The level sets of the first integral in M can be divided into three groups as well: $h < \psi(\alpha_1)$, $h = \psi(\alpha_1)$ and $\psi(\alpha_1) < h < \psi(\alpha_2)$, cf. the green, red and dark blue dashed lines in Fig. 6a. The corresponding (maximal) solutions of (8), whose first component runs from α_1 to α_2, are defined on bounded intervals of length

$$\int_{\alpha_1}^{\alpha_2} \frac{\mathrm{d}u}{|v_h^{\pm}(u)|} = \int_{\alpha_1}^{\alpha_2} \sqrt{\frac{\varphi(u)g(u)}{2(h - \psi(u))}}\,\mathrm{d}u < \infty,$$

for corresponding $h \in \mathbb{R}$. However these solutions do not yield traveling waves due to Lemma 5.1, since $\lim_{u \nearrow \alpha_2} v_h^+(u) = \infty$ for all h.

All orbits in R have a similar shape and correspond to a level set segment of $L_h(H)$ with $h > \psi(\alpha_2)$, cf. the light blue dashed line in Fig. 6a. Once again, Lemma 5.1 implies that they are not suitable to construct traveling waves.

If $c \geq c_1$, cf. Fig, 6a, the phase portrait of (8) changes qualitatively in L and in M due to the absence of the fixed points $(\alpha_1, \pm v_{\alpha_1})$. All orbits in L correspond to segments of $L_h(H)$ with $h \in \mathbb{R}$ and are unbounded in the first component. The orbits in M correspond to segments of $L_h(H)$ with $h < \psi(\alpha_2)$. They are all of the same type and are not suitable for the construction of traveling waves due to Lemma 5.1, cf. Fig. 6b.

Scenario II [Fig. 7]. In comparison with scenario I, the phase portraits (for both cases $c < c_1$ and $c_1 < c < \bar{c}$) change only within L, where one fixed point $(\bar{u}, 0)$, a cusp, is present, cf. Fig. 7. However, we see that all (non-constant) orbits in L are unbounded in the first component, so none of them can be used to construct a traveling wave. The trivial solution $u \equiv \bar{u}$ of (5) is the only traveling wave solution of (1).

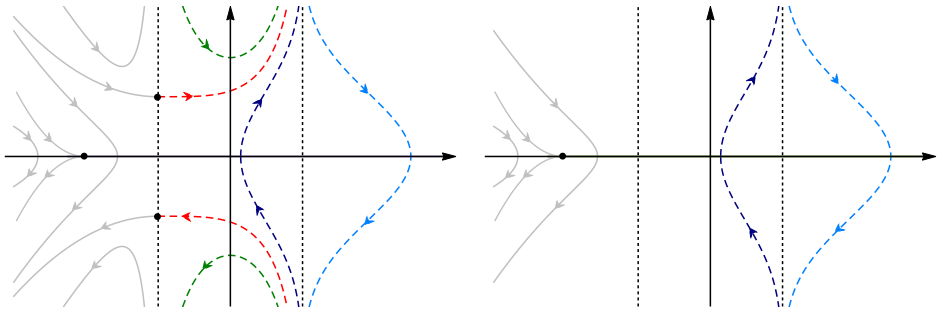

(a) $c \in (-\infty, c_1)$ (b) $c \in [c_1, \bar{c})$

FIGURE 7. Sketches of phase portraits for scenario II, i.e. $K = K_0(c)$

Scenario III [Fig. 8]. The picture in M and R is unchanged, but we will see that the orbits in L give rise to both smooth and non-smooth traveling waves.

We begin with the case $c < c_1$, cf. Fig. 8a–8c. Note that ψ has the following monotonicity properties: ψ increases strictly on $(-\infty, u_1)$ and attains a local maximum at u_1, decreases strictly on (u_1, u_2), takes a local minimum at u_2 and increases strictly on (u_2, ∞). Recall that ψ is continuous at α_1 since $\varphi \in L^1_{\mathrm{loc}}$ if $c < c_1$. The sign of $\psi(u_1) - \psi(\alpha_1)$, which depends on the choice of the parameter K, determines the qualitative behavior of the phase portrait of Fig. 8a-8c. Let us suppose for the moment that c is fixed such that $\alpha_1 \leq 0$, that is, $c \leq 4/7$. We define the differentiable function

$$F(K) \coloneqq \psi(u_1) - \psi(\alpha_1) = \int_{u_1(K)}^{\alpha_1} f_0(K,u)\,\varphi(u)\,\mathrm{d}u, \quad F\colon [K_0, K_{\alpha_1}] \to \mathbb{R},$$

where we write $f_0(K,u)$ to emphasize the K-dependence of f_0. By Leibniz' integral rule, the derivative of F with respect to K is given by

$$F'(K) = \int_{u_1(K)}^{\alpha_1} f_0'(K,u)\,\varphi(u)\,\mathrm{d}u - u_1'(K)\,f_0(K,u_1(K))\,\varphi(u_1(K)) > 0. \tag{43}$$

The positive sign follows from the fact that u_1 is by definition a zero of f_0, and moreover we have that $f_0'(K,u) = \partial_K f_0(K,u) = 1$ for all $K, u \in \mathbb{R}$. Thus F is strictly increasing. Furthermore, $F(K_0) < 0$ and $F(K_{\alpha_1}) > 0$, therefore F has a unique zero which we denote by $K_1 \in (K_0, K_{\alpha_1})$, and $F < 0$ in $[K_0, K_1)$, $F > 0$ in $(K_1, K_{\alpha_1}]$. If $4/7 < c < c_1$ then $\alpha_1(c) > 0$, and we can not apply Leibniz' rule on F since φ is not continuous at α_1. Note however, that F is still differentiable on $[K_0, K_{\alpha_1})$ and continuous at α_1, with $F(K_0) < 0$ and $F(K_{\alpha_1}) > 0$. Let $F_\varepsilon(K) \coloneqq \psi(u_1) - \psi(\alpha_1 - \varepsilon)$ for some sufficiently small $\varepsilon > 0$, which is defined on a subinterval $[K_0, K_\varepsilon] \subseteq [K_0, K_{\alpha_1}]$. By continuity we can choose ε small enough such that $F_\varepsilon(K_\varepsilon) > 0$. Then $F_\varepsilon' > 0$, which in turn shows that F is strictly increasing on $[K_0, K_{\alpha_1}]$ for all $c \in (-\infty, c_1)$, since ε can be chosen arbitrarily small.

If $K \in (K_0, K_1)$, cf. Fig. 8a, we find periodic orbits around the center $(u_2, 0)$ which are surrounded by a homoclinic orbit starting at the saddle $(u_1, 0)$. The periodic orbits, which correspond to energies $\psi(u_2) < h < \psi(u_1)$, yield smooth periodic traveling waves and the energy $h = \psi(u_1)$ corresponds to a homoclinic orbit, which gives rise to a smooth solitary wave, cf. Fig. 5b.

If $K = K_1$, cf. Fig. 8b, then $F(K) = 0$, which implies the existence of a heteroclinic orbit in $L^\pm$ connecting $(u_1, 0)$ with $(\alpha_1, \pm v_{\alpha_1})$; the corresponding energy is given by $h = \psi(u_1) = \psi(\alpha_1)$. The region in L inside these heteroclinic orbits and the invariant line at α_1 is filled with periodic orbits encircling $(u_2, 0)$, which correspond to level set segments of $L_h(H)$ with $\psi(u_2) < h < \psi(u_1)$. The two heteroclinic branches form a peaked solitary wave, cf. Fig. 9a. The periodic orbits yield smooth periodic waves cf. Fig. 5b.

If $K_1 < K < K_{\alpha_1}$, cf. Fig. 8c, there exists a heteroclinic orbit linking (α_1, v_{α_1}) with $(\alpha_1, -v_{\alpha_1})$ corresponding to the energy $h = \psi(\alpha_1) < \psi(u_1)$. This heteroclinic orbit bounds a region in L, which is filled with periodic orbits encircling $(u_2, 0)$ with energies $\psi(u_2) < h < \psi(\alpha_1)$. The heteroclinic orbit yields peaked periodic waves, the periodic orbits yield smooth periodic waves. The energy $h = \psi(u_1)$ corresponds to an orbit in L^+ which arises from $(u_1, 0)$ and becomes unbounded in the v-component as $u \nearrow \alpha_1$. This orbit combined with its counterpart in L^- yields a cusped solitary wave, cf. Fig. 9b, provided that the additional condition $c \in (c_0, c_1)$ is satisfied in

view of Lemma 5.1. For energies $\psi(\alpha_1) < h < \psi(u_1)$ we obtain periodic cusped traveling wave solutions if $c \in (c_0, c_1)$, again due to Lemma 5.1.

If $c_1 \leq c < \bar{c}$, cf. Fig. 8d, ψ has a pole at α_1 and we obtain a homoclinic orbit for energy $h = \psi(u_1)$ and periodic orbits for energies $\psi(u_2) < h < \psi(u_1)$. Hence we obtain a smooth solitary wave and smooth periodic traveling waves, cf. Fig. 5b. Energies other than these correspond to orbits which are unbounded in the u-component.

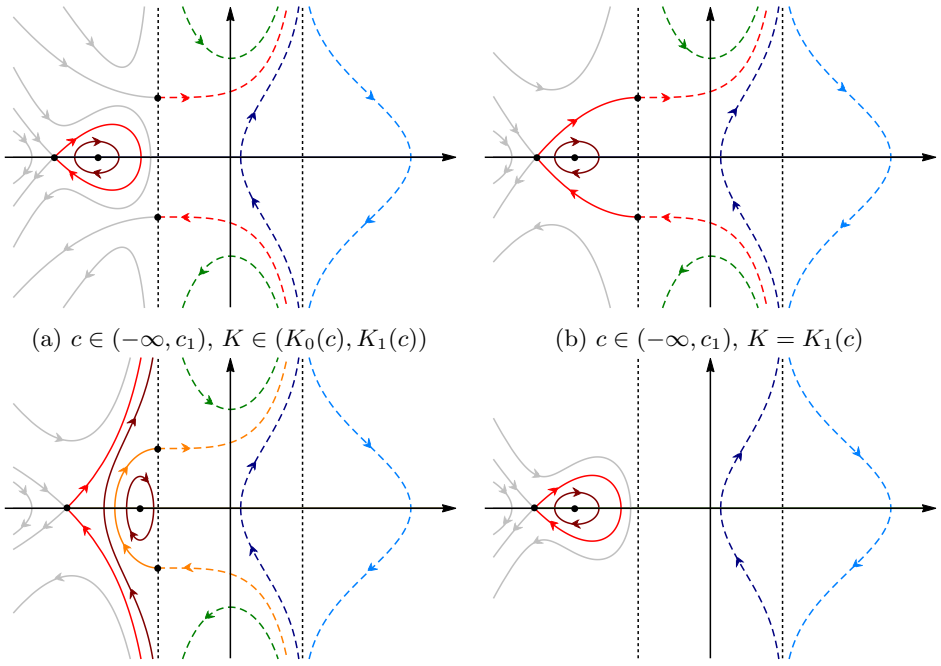

(a) $c \in (-\infty, c_1)$, $K \in (K_0(c), K_1(c))$ (b) $c \in (-\infty, c_1)$, $K = K_1(c)$

(c) $c \in (-\infty, c_1)$, $K \in (K_1(c), K_{\alpha_1}(c))$ (d) $c \in [c_1, \bar{c})$, $K \in (K_0(c), K_{\alpha_1}(c))$

FIGURE 8. Sketches of the phase portraits of scenario III: (8a)-(8d) yield smooth periodic waves, (8a) and (8d) yield smooth solitary waves, (8b) yields peaked solitary waves, (8c) yields peaked periodic and – provided that $c \in (c_0, c_1)$ – both periodic and solitary cusped traveling waves.

Remark 5.5. So far we have constructed non-smooth waves by combining orbits that correspond to one particular energy level h, see for instance Fig. 5 and Fig. 9. More precisely, these waves satisfy the following special version of property (TW2) in Proposition 18.

It holds that $\lambda(u^{-1}(N_g)) = 0$ and there exist $K, h \in \mathbb{R}$ such that

$$\begin{cases} (u')^2 = 2\dfrac{h - \psi(u)}{\varphi(u) g(u)} & \text{on all intervals } I_j \\ \\ u \to \alpha_i & \text{at finite endpoints of } I_j, \text{with } \alpha_i \in N_g. \end{cases} \tag{TW2'}$$

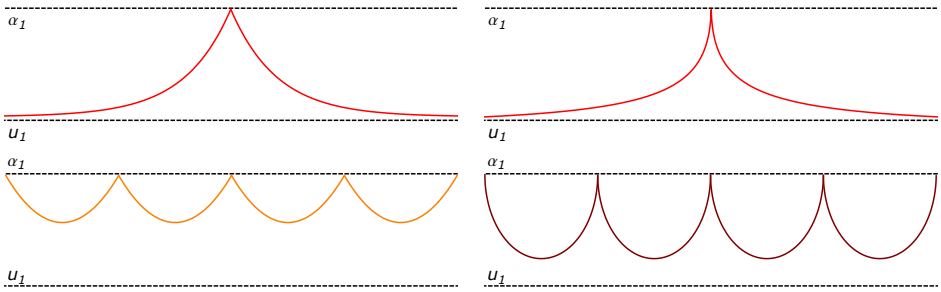

(a) (b)

FIGURE 9. Sketches of peaked (9a) and cusped (9b) traveling waves.

In particular all smooth traveling waves satisfy this property. Note however, that Proposition 4.1 also permits the combination of orbits which correspond to different energy levels. Scenarios IV and VII for instance yield rich collections of such combinations of solutions of system (8), see Fig. 11 and Fig 17c. To distinguish between these two types of traveling waves, we make the following definition:

Definition 5.6. A traveling wave solution of (1) is called an *elementary wave*, if (TW2') is satisfied. Otherwise we speak of a *composite wave*.

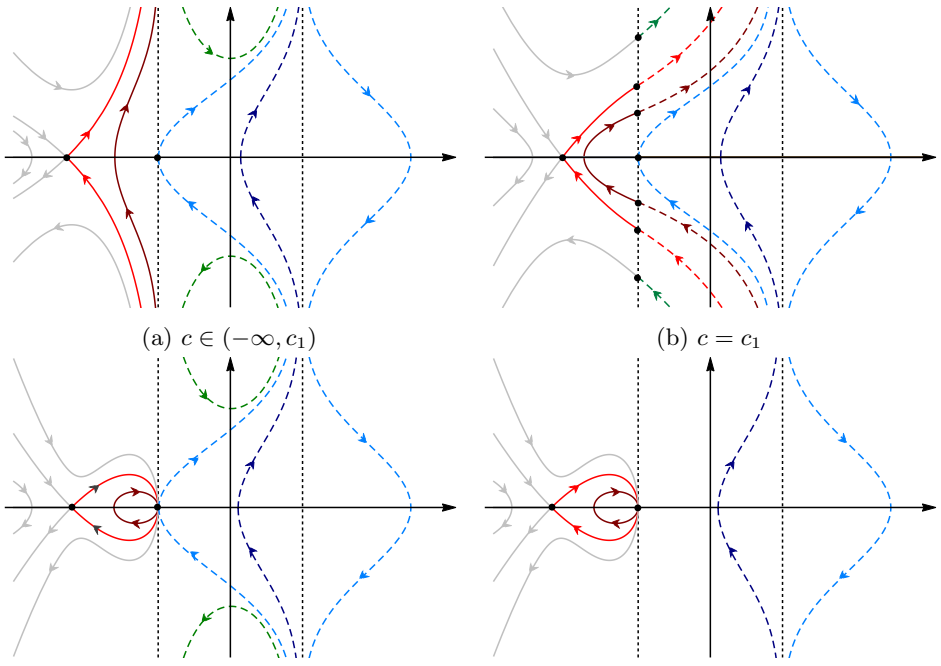

(a) $c \in (-\infty, c_1)$ (b) $c = c_1$

(c) $c \in (c_1, c_2)$ (d) $c \in [c_2, \bar{c})$

FIGURE 10. Sketches of phase portraits in scenario IV, i.e. $K = K_{\alpha_1}(c)$.

Scenario IV [Fig. 10]. We refer to the previous scenarios for the discussion of solution curves within the region R. Note that $\psi \in \mathcal{C}(\mathbb{R})$ if and only if $c < c_2$, cf. (35), due to the fact that f_0 vanishes in α_1.

Let us consider the region M first. For wave speeds $c \in (-\infty, c_2)\backslash\{c_1\}$, cf. Fig. 10a and Fig. 10c, we distinguish between three different types of level sets $L_h(H)$, similar as in the previous scenarios. The only qualitative difference is, that the upper branch of the M-segment of $L_h(H)$ for energy $h = \psi(\alpha_1)$ connects to a point on the u-axis, namely $(\alpha_1, 0)$. Indeed, if $c \neq c_1$ we find that

$$\lim_{u \searrow \alpha_1} (v_h^{\pm}(u))^2 = \lim_{u \searrow \alpha_1} 2\frac{\psi(\alpha_1) - \psi(u)}{\varphi(u)g(u)} = \lim_{u \searrow \alpha_1} \frac{f_0(u)}{B - 2Gu} = 0,$$

where we have used L'Hôpital's rule in the second equality. Furthermore we have that

$$\lim_{u \nearrow \alpha_2} (v_h^{\pm}(u))^2 = \lim_{u \nearrow \alpha_2} 2\frac{\psi(\alpha_1) - \psi(u)}{\varphi(u)g(u)} = \infty.$$

For $c \in [c_2, \bar{c})$, cf. Fig. 10d, each orbit in M corresponds to the M-segment of a level set $L_h(H)$ with $h < \psi(\alpha_2)$. These segments cross the u-axis and satisfy $\lim_{u \nearrow \alpha_2} v_h^{\pm}(u) = \pm\infty$. None of the orbits we considered so far are suitable for the construction of traveling waves by Lemma 5.1. We will analyse the case $c = c_1$ separately below.

Next we analyze the phase portraits within L. For the wave speeds $c < c_1$, cf. Fig. 10a, the function ψ is continuous on $\mathbb{R}$, increases strictly in the interval $(-\infty, u_1)$, takes a local maximum at $u = u_1$, decreases strictly on (u_1, α_1), has a local minimum at α_1 and increases on (α_1, ∞) with $\psi'(\alpha_1) = 0$. This yields, for the energy $h = \psi(u_1)$, a solution branch $\{(u, v_h^+(u))\colon u_1 < u < \alpha_2\}$ which connects to the saddle $(u_1, 0)$ with $\lim_{u \nearrow \alpha_1} v_h^+(u) = \infty$, cf. the upper red orbit in Fig. 10a. We can identify this orbit together with its counterpart in L^- with a cusped solitary wave, provided that $c \in (c_0, c_1)$, cf. Lemma 5.1. Energies $\psi(\alpha_1) < h < \psi(u_1)$ yield smooth orbits in L as indicated by the wine red line in Fig. 10a. The elementary traveling waves that correspond to theses orbits are periodic ones with cusps. There are no other solution curves possessing a bounded first component.

For $c \in (c_1, \bar{c})$, cf. Fig. 10c and Fig. 10d, the level $h = \psi(u_1)$ yields a heteroclinic orbit connecting $(u_1, 0)$ with $(\alpha_1, 0)$. This is obvious for $c \in (c_1, c_2)$, since in this case $(g\varphi)(u) \to \infty$ as $u \nearrow \alpha_1$, whereas $\psi(u_1) - \psi(u)$ stays bounded. For $c \in [c_2, \bar{c})$ we have that $\psi(u_1) - \psi(u) \to \infty$ as $u \nearrow \alpha_1$ and by applying de l'Hôpital's rule we obtain

$$\lim_{u \nearrow \alpha_1} 2\frac{\psi(u_1) - \psi(u)}{\varphi(u)g(u)} = \frac{f_0(\alpha_1)}{\frac{1}{B} - G\alpha_1} = 0.$$

The point $(\alpha_1, 0)$ is reached by a solution of (8) at some finite value of the moving frame variable s. Again this is obvious for $c \in (c_1, c_2)$ where ψ is continuous at α_1, because then φg has a finite improper integral and in particular

$$\int_{\alpha_1 - \varepsilon}^{\alpha_1} \frac{\mathrm{d}u}{|v_h^{\pm}(u)|} = \int_{\alpha_1 - \varepsilon}^{\alpha_1} \sqrt{\frac{\varphi(u)g(u)}{2(h - \psi(u))}}\,\mathrm{d}u < \infty$$

for sufficiently small $\varepsilon > 0$ such that $u_1 < \alpha_1 - \varepsilon$. If $c \in (c_2, \bar{c})$, we use that

$$\lim_{u \nearrow \alpha_1} \frac{\varphi(u)g(u)(\alpha_1 - u)}{2(h - \psi(u))} = \frac{\frac{1}{2}B - G\alpha_1 - C(\alpha_2 - \alpha_1)\alpha_1}{E(u_1 - \alpha_1)} \in (0, \infty), \tag{44}$$

which implies that the improper integral in (5.4.1) is again finite. Energies $h \in (\psi(\alpha_1), \psi(u_1))$ in case that $c \in (c_1, c_2)$, and energies $h \in (-\infty, \psi(u_1))$ in case that $c \in [c_2, \bar{c})$, yield homoclinic orbits of (8), cf. the wine red loop in Fig. 10c and Fig 10d. The corresponding solutions of (8) are defined on intervals of finite length.

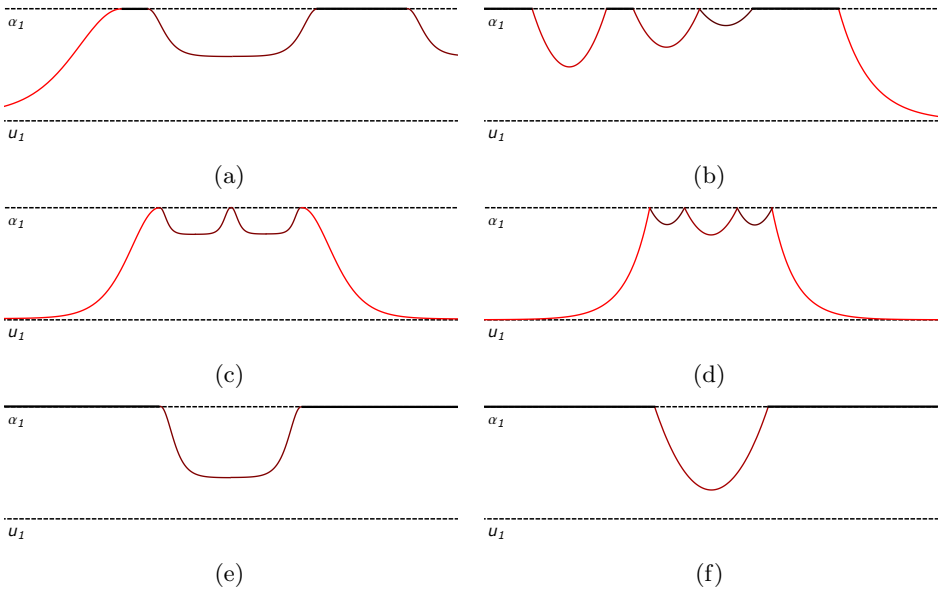

FIGURE 11. Some examples of composite waves constructed from orbits corresponding to scenario IV: smooth (11a) and peaked (11b) traveling wave solutions with plateaus at height α_1, smooth (11c) and peaked (11d) multi-crested solutions with decay, and smooth (11e) and non-smooth (11f) compactons.

Finally we analyze the case $c = c_1$, cf. Fig. 10b. We have that every point on the invariant line $\{u = \alpha_1\}$ of system (11) is a fixed point. Recall that the function f can be written as

$$f(u, v) = E(u - u_1)(u - \alpha_1) - G(u - \alpha_1)v^2$$

in this case, and that ψ is continuous on $\mathbb{R}$ in view of (35). It satisfies the same monotonicity properties as in the case $c < c_1$, but its graph is not smooth at the local minimum in α_1: the corresponding one-sided derivatives exist, but do not coincide. The function φg has a (finite) jump at α_1, since $1 - \theta\alpha_1 = 0$ if $c = c_1$ and therefore

$$(\varphi g)(u) = -C \operatorname{sgn}(u - \alpha_1) |u - \alpha_2|^{\theta\alpha_2 + 1}, \qquad u \in \mathbb{R} \setminus \{\alpha_1\},$$

for some constant C. Note, however, that the limit $v_h^{\pm}(\alpha_1^-) := \lim_{u \nearrow \alpha_1} v_h^{\pm}(u)$ is still defined. For $h = \psi(u_1)$ we obtain a heteroclinic orbit connecting $(u_1, 0)$ with the fixed point $(\alpha_1, v_h^+(\alpha_1^-))$. We obtain a peaked solitary wave by combining this orbit with its counterpart in L^-. Energies $h \in (\psi(\alpha_1), \psi(u_1))$ yield heteroclinic orbits in L which connect the fixed points $(\alpha_1, v_h^-(\alpha_1^-))$ with $(\alpha_1, v_h^+(\alpha_1^-))$ and cross the u-axis in some point $(u_h, 0)$. Due to the strict monotonicity of ψ and φg on (u_1, α_1) it is obvious, that $0 < v_{h_1}^+(\alpha_1^-) < v_{h_2}^+(\alpha_1^-)$ for $\psi(\alpha_1) < h_2 < h_1 \leq \psi(u_1)$.

Each one of these solution curves gives rise to a peaked periodic traveling wave of elementary type. By combining orbits of different energies, we obtain a rich collection of (not necessarily periodic) peaked waves. The orbits that correspond to energies $h > \psi(u_1)$ and $h < \psi(\alpha_2)$ are unbounded in u. The orbits in M correspond to energy levels $h < \psi(\alpha_2)$. All these orbits become unbounded in the second coordinate as u approaches α_2 from the left side. Therefore they are not useful for the construction of traveling waves in view of Lemma 5.1. For the sake of completeness we analyze their behavior as $u \searrow \alpha_1$. For $h = \psi(\alpha_1)$ we have that $\lim_{u\searrow\alpha_1} v_h^+(u) = 0$ – this orbit (and its reflection about the u-axis) is indicated by the light blue dashed line in Fig. 10b. Energies $h < \psi(\alpha_1)$ imply $\lim_{u\searrow\alpha_1} v_h^+(u) > 0$, and energies $\psi(\alpha_1) < h < \psi(\alpha_2)$ yield orbits indicated by a dark blue dashed line in Fig. 10b.

To conclude the discussion of scenario IV we observe that for any wave speed $-\infty < c < \bar{c}$ the constant solution $u \equiv \alpha_1$ is a classical solution of (5), since in this case $u' \equiv u'' \equiv 0$, $g(\alpha_1) = 0$, and $f_0(\alpha_1(c), K_{\alpha_1(c)}) = 0$. This enables the construction of composite waves, which are piecewise constant equal to α_1. We thereby obtain smooth and peaked traveling waves with plateaus and so-called compactons, cf. Fig. 11. Compactons are solitary waves with compact support in the sense that they take a constant value outside an interval of finite length; in other words a solitary wave of finite length.

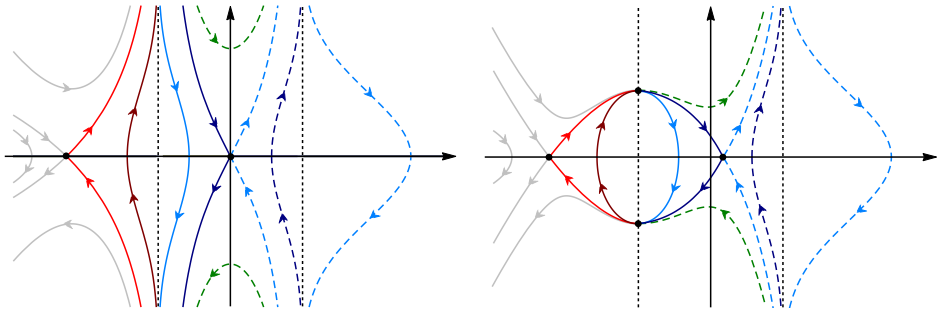

(a) $c \in (-\infty, c_1]$ (b) $c \in (c_1, \bar{c})$

FIGURE 12. Sketches of phase portraits in scenario V, i.e. $K \in (K_{\alpha_1}(c), K_{\alpha_2}(c))$.

Scenario V [Fig. 12]. We refer to the previous scenarios for the phase portraits within R. Recall that the set of fixed points of (11) consists of the two saddles $(u_1, 0) \in L$ and $(u_2, 0) \in M$ if $c \le c_1$. For larger wave speeds, i.e. $c \in (c_1, \bar{c})$, system (11) has the additional fixed points $(\alpha_1, \pm v_{\alpha_1})$.

First we consider the case $c \le c_1$, cf. Fig. 12a. We begin with the description of the orbits in L. If $c \ne c_1$, the function $\psi \in \mathcal{C}(\mathbb{R})$ decreases strictly on (u_1, α_1). We obtain a phase portrait similar as in scenario IV with $c \in (-\infty, c_1)$, cf. Fig. 10a. There are two kinds of relevant orbits: the two orbits with corresponding energy $h = \psi(\alpha_1)$, indicated by the red lines in Fig. 12a, and the orbits corresponding to energies $h \in (\psi(\alpha_1), \psi(u_1))$, which are indicated by wine red lines in Fig. 12a. These orbits are suitable for the construction of traveling waves if $c \in (c_0, c_1)$. The situation is similar in the case $c = c_1$. The only difference is, that the orbits of the latter type (wine red) correspond to energies $h < \psi(u_1)$.

Next we describe the orbits in M. Let us again first assume that $c \neq c_1$. Observe that $\psi \in \mathcal{C}(\mathbb{R})$ decreases strictly on (α_1, u_2), takes a local minimum in u_2 and increases strictly on (u_2, α_2). There are two kinds of relevant orbits in M, whose second components become unbounded at α_1: the two orbits corresponding to $h = \psi(u_2)$, indicated by the dark blue lines in Fig. 12a, and the orbits corresponding to $\psi(u_2) < h < \psi(\alpha_1)$, indicated by the light blue line. The corresponding elementary traveling waves are solitary and periodic anti-cusps, cf. Fig 14a. The situation is similar in the case $c = c_1$. The only difference is, that the orbits of the latter type (light blue) correspond to energies $h > \psi(u_2)$. We may combine orbits in L and M to obtain composite waves, such as steep wavefronts, see Fig. 13b.

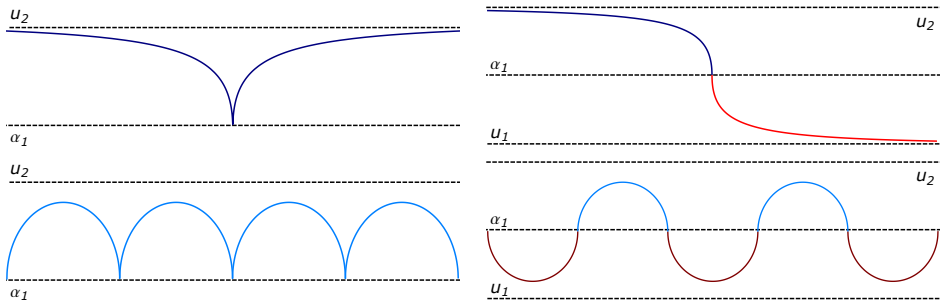

(a) (b)

FIGURE 13. Traveling waves constructed from orbits corresponding to the phase portrait in Scenario V, Fig. 12a: Fig. 13a shows solitary and periodic anti-cusped waves. Fig. 13b shows composite waves: a steep wave front and a periodic composition.

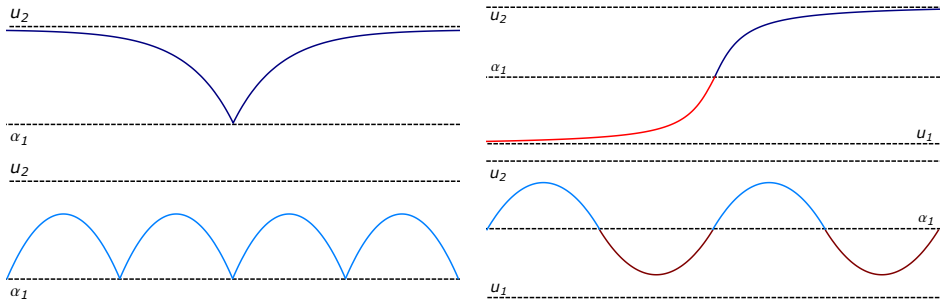

(a) (b)

FIGURE 14. Traveling waves constructed from orbits corresponding to the phase portrait in Scenario V, Fig. 12b: Fig. 14a shows solitary and periodic anti-peaked waves. Fig. 14b shows composite waves: a wave front and a periodic composition.

If $c_1 < c < \bar{c}$, cf. Fig. 12b, then (11) has the additional fixed points $(\alpha_1, \pm v_{\alpha_1})$ which are stable and unstable nodes. The suitable M^+-segments of the level-sets

$L_h(H)$ with $h \geq \psi(u_2)$ in M and the L^+-segments of $L_h(H)$ with $h \leq \psi(u_1)$ in L reach the point (α_1, v_{α_1}) as $u \to \alpha_1$ and the corresponding solutions of (8) reach this point as the moving frame variable approaches some finite value s_0. Therefore we obtain elementary waves with peaks, cf. Fig. 14a. Moreover, we can construct a large variety of composite waves, e.g. wave fronts, see Fig. 14b.

Scenario VI [Fig. 15]. We refer to the previous scenario for the description of the regions L and R, and proceed with the discussion for the region M.

Let $c \leq c_1$, cf. Fig. 15a, and assume for the moment that $c \neq c_1$. Observe that $\psi \in \mathcal{C}(\mathbb{R})$ decreases strictly on (α_1, α_2). There are two types of suitable orbits in M. The two orbits corresponding to $h = \psi(\alpha_2)$ reaching the nilpotent fixed point $(\alpha_2, 0)$ of (11), which are indicated by the dark blue lines, and the orbits corresponding to $h \in (\psi(\alpha_2), \psi(\alpha_1))$; one of them is indicated by a light blue line. All these orbits are suitable for the construction of traveling waves, provided that $c > c_0$ is satisfied in view of Lemma 5.1. We observe that (maximal) solutions of (8) in M, which correspond to the energy $h = \psi(\alpha_2)$, are defined on a bounded interval I of length δ. Similar as in (44) it holds that

$$\lim_{u \nearrow \alpha_2} \frac{\varphi(u)g(u)(\alpha_2 - u)}{2(h - \psi(u))} = \frac{\frac{1}{2}B - G\alpha_2}{E(u_1 - \alpha_2)} \in (0, \infty),$$

hence δ is given by

$$\delta = \int_{\alpha_1}^{\alpha_2} \frac{\mathrm{d}u}{|v_h^{\pm}(u)|} = \int_{\alpha_1}^{\alpha_2} \sqrt{\frac{\varphi(u)g(u)}{2(h - \psi(u))}}\, \mathrm{d}u < \infty.$$

The situation is similar in the case $c = c_1$, the difference being that the orbits of the light blue type correspond to energies $h > \psi(\alpha_1)$. Let now $c \in (c_1, \bar{c})$, cf. Fig. 15b. Similar as in the previous case we obtain that all orbits in M^+ are connected to (α_1, v_{α_1}).

We observe that the constant function $u \equiv \alpha_2$ is a classical solution of (5) for all wave speeds $c < \bar{c}$. We may therefore construct traveling waves of (1), which are piecewise constant. For instance, there exist *anti-cuspcompactons* for $c_0 < c \leq c_1$, and *anti-peakompactons* for $c_1 < c < \bar{c}$. These solitary waves have the finite length 2δ with a cusp or peak respectively at their trough, see Fig. 17a.

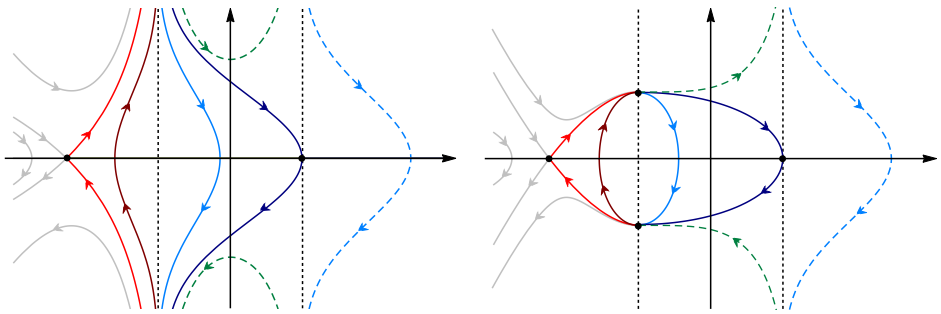

(a) $c \in (-\infty, c_1]$ (b) $c \in (c_1, \bar{c})$

FIGURE 15. Sketches of phase portraits in scenario VI, i.e. $K = K_{\alpha_2}(c)$.

Scenario VII [Fig. 16]. We refer to the previous scenario for the discussion of L.

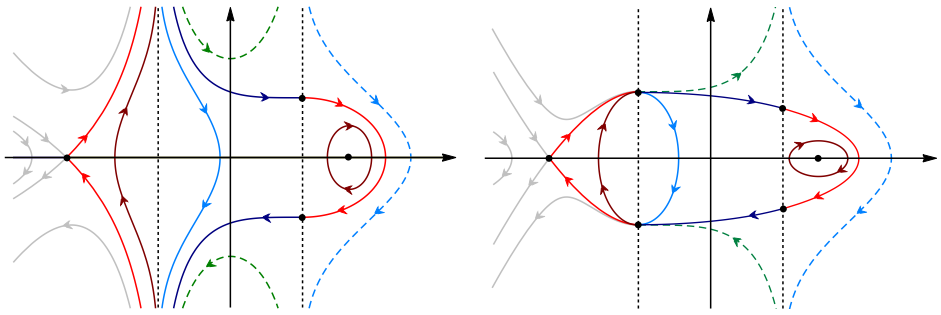

(a) $c \in (-\infty, c_1]$ (b) $c \in (c_1, \bar{c})$

FIGURE 16. Sketches of phase portraits in scenario VII, i.e. $K > K_{\alpha_2}(c)$.

The restriction of the phase portrait to M is similar as in the previous scenario for all $-\infty < c < \bar{c}$. The main difference is that the orbits corresponding to $h = \psi(\alpha_2)$ reach the points $(\alpha_2, \pm v_{\alpha_2})$, which are saddles of (11). We may use these orbits for the construction of periodic traveling waves with peaked crests and cusped troughs, if $c_0 < c \leq c_1$, or waves where both crests and troughs are peaked, if $c_1 < \bar{c}$, cf. Fig 17b.

The situation in R is differs from all the other scenarios. Energy $h = \psi(\alpha_2)$ yields a heteroclinic orbit connecting (α_2, v_{α_2}) with $(\alpha_2, -v_{\alpha_2})$. It crosses the u-axis at some point to the right of the center $(u_2, 0)$. The region bounded by this orbit and the vertical line $\{u = \alpha_2\}$ is filled with periodic orbits corresponding to energies $\psi(u_2) < h < \psi(\alpha_2)$ encircling the center $(u_2, 0)$. Energies $h > \psi(\alpha)$ yield orbits, which are not suitable for the construction of traveling waves.

Scenario VII enables the construction of composite waves, where orbits from all three regions L, M and R with different energy levels are combined. We sketch an example of such a composite wave in Fig. 17c.

5.4.2. *Case $c = \bar{c}$.* The quadratic polynomial g has one double root α and φ given by (32) is an integrating factor for (11), which satisfies

$$\lim_{u \nearrow \alpha} \varphi(u) = \lim_{u \to -\infty} \varphi(u) = \lim_{u \to \infty} \varphi(u) = \infty, \quad \lim_{u \searrow \alpha} \varphi(u) = 0.$$

The corresponding first integral H is defined on $\mathbb{R}^2 \setminus (\{\alpha\} \times \mathbb{R})$. The vertical line $\{u = \alpha\}$ is an invariant set of system (11), which separates the (u, v)-plane into the two regions

$$L := \{(u, v) \colon -\infty < u < \alpha\} \quad \text{and} \quad R := \{(u, v) \colon \alpha < u < \infty\}.$$

We observe that φ vanishes faster then any polynomial as $u \searrow \alpha$. This implies that orbits in R, which become unbounded in the v-component as $u \searrow \alpha$ are not suitable for the construction of traveling waves. Indeed, similarly as in Lemma 5.1, we see that the existence interval of these orbits is finite, but

$$\int_{\alpha}^{\alpha+\varepsilon} v_h^+(u)\, \mathrm{d}u = \infty,$$

for any $\varepsilon > 0$ and all $h > 0$. Therefore the second component of the corresponding solution curves in R are not locally square integrable in view of (17).

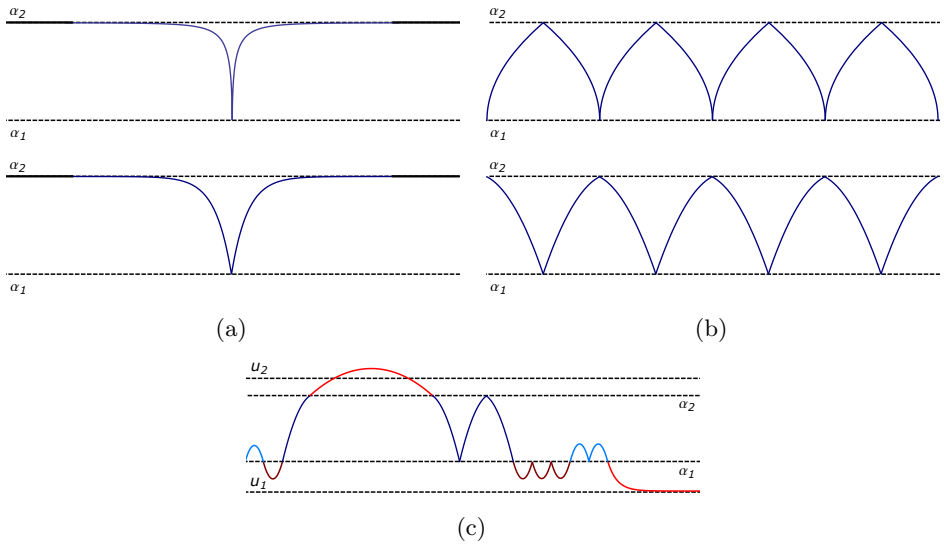

FIGURE 17. In Fig. 17a we see sketches of an anti-cusped and an anti-peaked solitary wave taking the constant value α_2 outside a bounded interval - they correspond to the dark blue lines in Fig. 15a and 15b, respectively. The first image in Fig. 17b shows a periodic wave with peaked crests and cusped troughs. In the second sketch in Fig. 17b we see a periodic wave with peaked crests and troughs. These waves correspond to the dark blue lines in Fig. 16a and 16b, respectively. In Fig. 17c we see an example of a composite wave constructed from orbits of different energy levels in Fig. 16b .

In the following we study the solutions of (8) for increasing values of K. We distinguish between five scenarios , cf. I-V in Table 1.

Scenarios I and II [Fig. 18]. These scenarios do not yield traveling waves apart from the trivial constant wave $u \equiv \bar{u}$ in scenario II. The L-segment of any (nonempty) level-set $L_h(H)$ is unbounded in u. The orbits in R, which correspond to R-segments of $L_h(H)$ for $h > 0$, are bounded in u but the second components of these solution curves are not locally square integrable and therefore not suitable for the construction of traveling waves.

Scenario III [Fig. 19a]. We refer to scenarios I and II for the phase portrait in R. The phase portrait in L looks similar as in scenario III in Section 5.4 for wave speeds $c \in [c_1, \bar{c})$. We find a homoclinic orbit of (8) corresponding to the $L_h(H)$-segment with $h = \psi(u_1)$, which yields a smooth solitary wave. Energies $h \in (\psi(u_2), \psi(u_1))$ yield periodic orbits encircling the center u_2, which correspond to smooth periodic waves, cf. Fig. 5b.

Scenario IV [Fig. 19b]. The situation in R is similar as in the previous scenarios. The restriction of phase portrait to L as well as the corresponding traveling wave solutions are similar as in scenario IV in Section 5.4 with $c \in [c_2, \bar{c})$, cf. Fig. 10d and Fig. 11b. The heteroclinic orbits indicated by red lines correspond to the energy

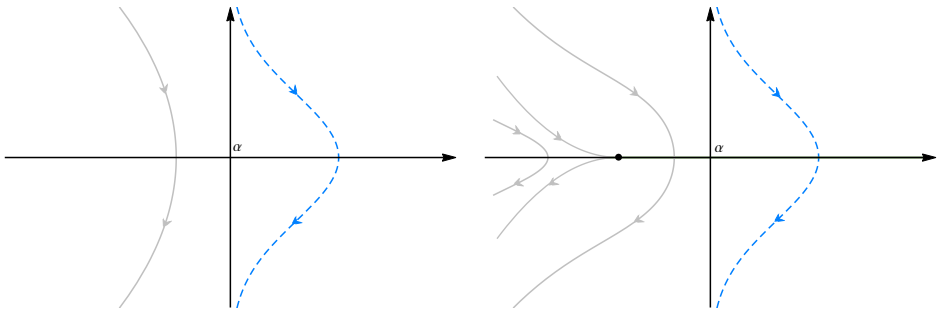

(a) $K < K_0$ (b) $K = K_0$

FIGURE 18. Sketches of phase portraits in scenarios I and II.

$h = \psi(u_1)$, whereas the homoclinic orbits of system (11), indicated by a wine-red line, correspond to energies $h < \psi(u_1)$.

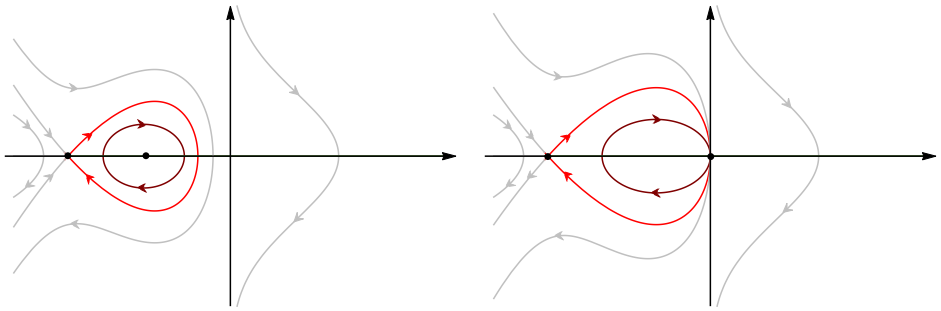

(a) $K_0 < K < K_\alpha$ (b) $K = K_\alpha$

FIGURE 19. Sketches of phase portraits in scenarios III and IV.

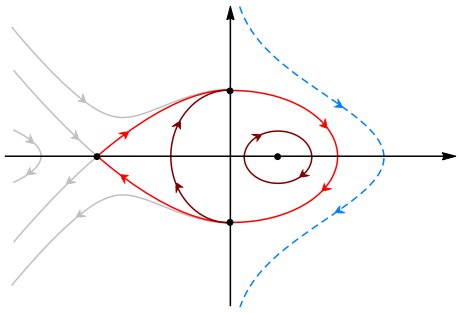

FIGURE 20. Sketches of the phase portrait corresponding to scenario V, i.e. $K > K_\alpha$.

Scenario V [Fig. 20]. For this choice of the parameter K, systems (8) and (11) have a saddle in $(u_1, 0)$ and a center in $(u_2, 0)$. Additionally, system (11) the two non-hyperbolic fixed points $(\alpha, \pm v_\alpha)$.

We describe the phase portrait in L. Only the energies $h \leq \psi(u_1)$ yield orbits that are bounded in the first coordinate. Let $h = \psi(u_1)$. The branches $\{(u, v_h^{\pm}(u))\colon u_1 < u < \alpha\}$ link $(u_1, 0)$ with $(\alpha, \pm v_\alpha)$. The corresponding orbits of (11) are indicated by the red lines in the left half-plane in Fig. 20. The energies $h < \psi(u_1)$ correspond to heteroclinic orbits from $(\alpha, -v_\alpha)$ to (α, v_α), cf. the wine red orbit in the left half-plane in Fig. 20. The following types of elementary waves can be obtained: peaked solitary and peaked periodic traveling waves.

Next we discuss the phase portrait in R. The energy $h = 0$ yields a heteroclinic orbit from $(\alpha, -v_\alpha)$ to (α, v_α), which is indicated by the red line in the right half-plane in Fig. 20. Energies $h \in (\psi(u_2), 0)$ correspond to periodic orbits around the center in $(u_2, 0)$. Thus we obtain smooth periodic waves and an anti-peaked periodic wave. The orbits that correspond to energies $h > 0$ are not suitable for the construction of traveling waves.

Remark 5.7 (Cantor waves)**.** Let us point out that it is possible to obtain composite waves of fractal type, for instance Cantor waves as indicated in Fig. 21, using constructions based on iterative schemes. Such fractal functions appear also as traveling wave solutions of the CH equation, cf. [31]. In order to construct the aforementioned Cantor wave, we use a suitable collection of either cusp or peak elements with the property that for each value $\delta \in (0, \delta_0]$, with $\delta_0 > 0$, there exists an element such that the corresponding solutions of (8) passing through this element are defined on a maximal interval of existence of length δ. In the following we demonstrate that such collections do indeed exist e.g. in scenarios V – VII of Table 1. For $c \in (c_0, c_1)$ and $K > K_{\alpha_1}(c)$ we can construct cusped as well as anti-cusped Cantor waves; for every $c \in (c_1, \bar{c})$ and $K > K_{\alpha_1}(c)$ we obtain peaked as well as anti-peaked Cantor waves. We carry out the details only for cusped waves, the other cases being similar.

Fix $h_0 \in (\psi(\alpha_1), \psi(u_1))$ and consider the cusp component in L of the level set $L_{h_0}(H)$, e.g. the orbit indicated by the wine red line in Fig. 16a. We have already shown that solutions of (8) passing through this curve are defined on an interval of finite length $2\delta_0 > 0$ with

$$\delta_0 = \int_{u_0(h_0)}^{\alpha_1} \frac{\mathrm{d}u}{v_{h_0}^+(u)},$$

where $u_0(h_0)$ denotes the unique point in (u_1, α_1), at which ψ takes the value h_0. The collection of cusp components corresponding to energies $\psi(\alpha_1) < h < h_0$ fills the entire region between the h_0-curve and the vertical line $\{u = \alpha_1\}$. Let

$$\delta\colon (\psi(\alpha_1), h_0] \to \mathbb{R}, \quad \delta(h) \coloneqq \int_{u_0(h)}^{\alpha_1} \frac{\mathrm{d}u}{v_h^+(u)},$$

where $u_0(h)$ denotes the unique point in $[u_0(h_0), \alpha_1)$, at which ψ takes the value h. Then $\delta(h_0) = \delta_0$ and it is clear that δ is positive. We will show that

$$\delta(h) \to 0 \quad \text{as} \quad h \to \psi(\alpha_1), \tag{45}$$

that is, the maximal existence interval of a cusp element can be arbitrarily small. It follows from the continuity of the functions g, φ and ψ on $[u_0(h_0), \alpha_1)$, that $\delta\colon (\psi(\alpha_1), h_0] \to (0, \delta_0]$ is onto. This guarantees that the collection of cusp elements with energies $h \in (\psi(\alpha_1), h_0]$ is suitable for the construction of a composite wave as illustrated in Fig. 21b, where the preimage of $\{\alpha_1\}$ under this wave is a Cantor set.

In order to show (45), we fix $h \in (\psi(\alpha_1), h_0]$ and split the integral $\delta(h)$ into two parts:

$$\delta(h) = \delta_1(h) + \delta_2(h) = \int_{u_0(h)}^{u^*(h)} \frac{\mathrm{d}u}{v_h^+(u)} + \int_{u^*(h)}^{\alpha_1} \frac{\mathrm{d}u}{v_h^+(u)},$$

where $u^*(h) \coloneqq u_0(h) + (\alpha_1 - u_0(h))/2$. Then

$$\delta_2(h) \leq \frac{\alpha_1 - u^*(h)}{v_h^+(u^*(h))} \leq \frac{\alpha_1 - u^*(h)}{v_{h_0}^+(u^*(h_0))} \to 0 \quad \text{as} \quad h \to \psi(\alpha_1),$$

since clearly $u^*(h) \to \alpha_1$ for $h \to \psi(\alpha_1)$. In order to see that also $\delta_1(h) \to 0$ as $h \to \psi(\alpha_1)$, we observe that $1/v_h^+(u) \in \Theta(1/\sqrt{u - u_0(h)})$ for $u \searrow u_0(h)$. Therefore, there exists a constant $\mathrm{C} > 0$ such that

$$\delta_1(h) \leq \mathrm{C} \int_{u_0(h)}^{u^*(h)} \frac{\mathrm{d}u}{\sqrt{u - u_0(h)}} = 2\mathrm{C}\sqrt{u^*(h) - u_0(h)} \to 0 \quad \text{as} \quad h \to \psi(\alpha_1),$$

since $u_0(h) \to \alpha_1$ in this limit. Thus we have shown that the maximal existence intervals of cusp elements (and similarly for peak elements) can be arbitrarily small. More precisely, the length of such intervals can take any value in $(0, 2\delta_0]$. Note that this implies in particular that equation (1) admits peaked and cusped periodic traveling waves of arbitrarily small wave length.

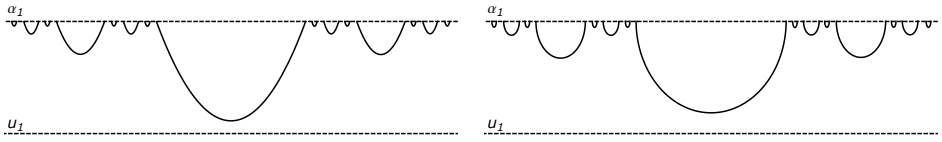

(a) (b)

FIGURE 21. Sketches of Cantor waves with peak elements (a) and cusp elements (b).

6. **Main results.** In this section we summarize our main results, based on the comprehensive phase plane analysis of the integrable system (8) in Section 5. To this end, let us briefly recall that solution curves of (8) correspond to the level sets $L_h(H)$ of the first integral H. We denote the energy level of each solution curve by $h \in \mathbb{R}$. Note that $H(u, 0) = \psi(u)$ is defined in (14), while $u_{1,2}$ and $\alpha_{1,2}$ denote the real zeros of the quadratic polynomials g and f_0, see Section 5.1. We review the following "critical" values of the parameters c and K: $\bar{c}$ is the bifurcation point of the double root α of $g(u)$, cf. (25); for every c, the value $K_0(c)$ is the bifurcation point of the double root $\bar{u}$ of $f_0(u)$, cf. (24); for $c \leq \bar{c}$, the value $K_1(c)$ is defined in Section 5.4.1, Scenario III, and the values $K = K_{\alpha_i}(c)$, $i \in \{1, 2\}$, are the ones at which the root $\alpha_i(c)$ of g coincides with the root $u_2(c, K)$ of f_0, cf. (29); c_1 denotes the wave speed at which fixed points on the invariant line $\{u = \alpha_1\}$ of system (11) bifurcate, cf. (31), it is the supremum over all $c \leq \bar{c}$ with $K \neq K_{\alpha_1}$ such that ψ is still continuous; c_2 is the supremum over all $c \leq \bar{c}$ such that ψ is still continuous in the case that $K = K_{\alpha_1}$, cf. (35); c_0 is the infimum over all $c \leq \bar{c}$ such that solution candidates, which satisfy (TW1), (TW2) and contain cusped-type singularities at the value $u = \alpha_1$, do also satisfy (TW3), cf. (37); it holds that $c_0 < c_1 < c_2 < \bar{c}$, and for fixed $c < \bar{c}$ we have that $K_0 < K_1 < K_{\alpha_1} < K_{\alpha_2}$.

Our first theorem classifies all elementary traveling waves of (1), that is, traveling waves constructed from orbits corresponding to a single energy level h, cf. Definition 5.6.

Theorem 6.1 (Elementary waves)**.** *Every elementary traveling wave u of (1) belongs to one of the following types:*

(i) Smooth periodic. *They appear if and only if the parameters c, K and h satisfy one of the following relations.*
- *(a)* $c > \bar{c}$, *and* $K > K_0(c)$, $\psi(u_2) < h < \psi(u_1)$ [Fig. 5]
- *(b)* $c = \bar{c}$, *and* $K_0(c) < K < K_\alpha(c)$, $\psi(u_2) < h < \psi(u_1)$ [Fig. 19a]
- *(c)* $c = \bar{c}$, *and* $K > K_\alpha(c)$, $\psi(u_2) < h < 0$ [Fig. 20]
- *(d)* $c < \bar{c}$, *and* $K_0(c) < K < K_{\alpha_1}(c)$, $\psi(u_2) < h < \psi(u_1)$ [Fig. 8]
- *(e)* $c < \bar{c}$, *and* $K > K_{\alpha_2}(c)$, $\psi(u_2) < h < \psi(\alpha_2)$ [Fig. 16]
- *(f)* $c_1 < c \le \bar{c}$, *and* $K = K_{\alpha_1}(c)$, $\psi(\alpha_1) < h < \psi(u_1)$ *if* $c_1 < c < c_2$ *and* $h < \psi(u_1)$ *if* $c_2 < c \le \bar{c}$ [Fig. 10c,10d]*; the solutions are* $\mathcal{C}^1(\mathbb{R})$

(ii) Smooth solitary. *They appear if and only if the parameters c, K and h satisfy one of the following relations.*
- *(a)* $c > \bar{c}$, *and* $K > K_0(c)$, $h = \psi(u_1)$ [Fig. 5]
- *(b)* $c_1 \le c \le \bar{c}$, *and* $K_0(c) < K < K_{\alpha_1}(c)$, $h = \psi(u_1)$ [Fig. 8d, 19a]
- *(c)* $c < c_1$, *and* $K_0(c) < K < K_1(c)$, $h = \psi(u_1)$ [Fig. 8a]
- *(d)* $c_1 < c \le \bar{c}$, *and* $K = K_{\alpha_1}(c)$, *for* $h = \psi(\alpha_1)$ [Fig. 10c,10d]

(iii) Peaked solitary. *They appear if and only if the parameters c, K and h satisfy one of the following relations.*
- *(a)* $c = \bar{c}$, *and* $K > K_\alpha$, $h = \psi(u_1)$ [Fig. 20]
- *(b)* $c_1 < c < \bar{c}$, *and* $K > K_{\alpha_1}(c)$, $h = \psi(u_1)$ [Fig. 12b, 15b, 16b]
- *(c)* $c = c_1$, $K = K_{\alpha_1}(c)$ *and* $h = \psi(u_1)$ [Fig. 10b]
- *(d)* $c < c_1$, *and* $K = K_1(c)$, $h = \psi(u_1)$ [Fig. 8b]

(iv) Anti-peaked solitary. *They appear if and only if the parameters c, K and h satisfy* $c_1 < c < \bar{c}$, *and* $K_{\alpha_1}(c) < K < K_{\alpha_2}(c)$, $h = \psi(u_2)$ [Fig. 12b].

(v) Peaked periodic. *They appear if and only if the parameters c, K and h satisfy one of the following relations.*
- *(a)* $c = \bar{c}$, *and* $K > K_\alpha$, $h < \psi(u_1)$ [Fig. 20]
- *(b)* $c_1 < c < \bar{c}$, *and* $K > K_{\alpha_1}(c)$, $h < \psi(u_1)$ [Fig. 12b, 15b, 16b]
- *(c)* $c = c_1$, *and* $K = K_{\alpha_1}(c)$, $\psi(\alpha_1) < h < \psi(u_1)$ [Fig. 10b]
- *(d)* $c < c_1$, *and* $K_1(c) < K < K_{\alpha_1}(c)$, $h = \psi(\alpha_1)$ [Fig. 8c]

(vi) Anti-peaked periodic. *They appear if and only if the parameters c, K and h satisfy one of the following relations.*
- *(a)* $c_1 < c < \bar{c}$, *and* $K_{\alpha_1}(c) < K < K_{\alpha_2}(c)$, $h > \psi(u_2)$ [Fig. 12b]
- *(b)* $c_1 < c < \bar{c}$, *and* $K \ge K_{\alpha_2}(c)$, $h > \psi(\alpha_2)$ [Fig. 15b, 16b]
- *(c)* $c < \bar{c}$, *and* $K > K_{\alpha_2}(c)$, $h = \psi(\alpha_2)$ [Fig. 16b]

(vii) Cusped solitary. *They appear if and only if the parameters c, K and h satisfy one of the following relations.*
- *(a)* $c_0 < c < c_1$, *and* $K_1(c) < K \le K_{\alpha_1}(c)$, $h = \psi(u_1)$
- *(b)* $c_0 < c \le c_1$, *and* $K > K_{\alpha_1}(c)$, $h = \psi(u_1)$

(viii) Cusped periodic. *They appear if and only if the parameters c, K and h satisfy one of the following relations.*
- *(a)* $c_0 < c < c_1$, *and* $K_1(c) < K \le K_{\alpha_1}(c)$, $\psi(\alpha_1) < h < \psi(u_1)$ [Fig. 8c, 10a]
- *(b)* $c_0 < c < c_1$, *and* $K > K_{\alpha_1}(c)$, $\psi(\alpha_1) < h < \psi(u_1)$ [Fig. 12a, 15a, 16a]
- *(c)* $c = c_1$, *and* $K > K_{\alpha_1}(c)$, $h < \psi(u_1)$

(ix) Anti-cusped periodic. *They appear if and only if the parameters c, K and h satisfy one of the following relations.*
  (a) $c_0 < c < c_1$, *and* $K_{\alpha_1}(c) < K < K_{\alpha_2}(c)$, $\psi(u_2) < h < \psi(\alpha_1)$ [Fig. 12a]
  (b) $c_0 < c < c_1$, *and* $K \geq K_{\alpha_2}(c)$, $\psi(\alpha_2) < h < \psi(\alpha_1)$ [Fig. 15a, 16a]
  (c) $c = c_1$, *and* $K_{\alpha_1}(c) < K < K_{\alpha_2}(c)$, $h > \psi(u_2)$
  (d) $c = c_1$, *and* $K \geq K_{\alpha_2}(c)$, $h > \psi(\alpha_2)$

(x) Anti-cusped solitary. *They appear if and only if the parameters c, K and h satisfy* $c_0 < c \leq c_1$, *and* $K_{\alpha_1}(c) < K < K_{\alpha_2}(c)$, $h = \psi(u_2)$ [Fig. 12a, 15a]

(xi) Periodic waves with peaked crests and cusped troughs. *They appear if and only if the parameters c, K and h satisfy* $c_0 < c \leq c_1$, *and* $K > K_{\alpha_2}(c)$, $h = \psi(\alpha_2)$. [Fig. 16a]

(xii) Periodic waves with peaked crests and troughs. *They appear if and only if the parameters c, K and h satisfy* $c_1 < c < \bar{c}$, *and* $K > K_{\alpha_2}(c)$, $h = \psi(\alpha_2)$. [Fig. 16b]

The wave profiles of periodic elementary waves have exactly one maximum and one minimum per period, while the wave profiles of solitary elementary waves have a unique maximum or minimum. The smooth, peaked and cusped solitary waves decay exponentially to the constant $u = u_1$ at infinity, while the anti-peaked and anti-cusped solitary waves tend exponentially to the constant $u = u_2$. The cusps always have the value $u = \alpha_1$, while the peaks have the value $u = \alpha_1$ except for situations (xi) and (xii) where the peaks take the value $u = \alpha_2$. Anti-peaks take either the value α_1 or α_2.

We now emphasize certain types of composite waves of special interest. The next theorem deals with wavefronts, which are composite waves consisting of two components: one half of a solitary peak and one half of a solitary anti-peak, or vice versa. Steep wavefronts consist of a solitary cusp component and a solitary anti-cusp component, cf. Fig. 12–14. Moreover, we consider "fast" wavefronts, which attain their maximum at a finite value of the moving frame variable, by combining a solitary cusp or peak component with a solitary anti-cusp or anti-peak component, cf. Fig. 15, 17a.

Theorem 6.2 (Wavefronts)**.** *The appearance of wavefronts is characterized as follows:*

(i) Wavefronts *occur if and only if* $c_1 < c < \bar{c}$ *and* $K_{\alpha_1}(c) < K < K_{\alpha_2}(c)$ *for* $h_i = \psi(u_i)$, $i = 1, 2$. [Fig. 12b].

(ii) Steep wavefronts *occur if and only if* $c_0 < c \leq c_1$ *and* $K_{\alpha_1}(c) < K < K_{\alpha_2}(c)$ *for* $h_i = \psi(u_i)$, $i = 1, 2$. [Fig. 12a].

(iii) Fast wavefronts *occur if and only if* $c_1 < c < \bar{c}$ *and* $K = K_{\alpha_2}(c)$ *for* $h_i = \psi(u_i)$, $i = 1, 2$. [Fig. 15b].

(iv) Fast steep wavefronts *occur if and only if* $c_0 < c \leq c_1$ *and* $K = K_{\alpha_2}(c)$ *for* $h_i = \psi(u_i)$, $i = 1, 2$. [Fig. 15a].

The profile of wavefronts (i) and (ii) tends to its maximal value $u = u_2$ and to its minimal value $u = u_1$ as $s \to \pm\infty$, while fast wavefronts attain their maximal value $u = \alpha_2$ at a finite value of the moving frame variable s. The slope of steep wavefronts becomes infinite precisely at the value $u = \alpha_1$, while the slope of a wavefront remains bounded everywhere.

Our last theorem classifies composite waves with constant components of finite or infinite length. In particular, there exist waves with plateaus and so-called compactons, which are solitary waves with compact support.

Theorem 6.3 (Compactons, plateau waves, multicrests, multipeaks)**.** *Traveling waves of* (1) *involving constant components can occur if* $c_0 < c \leq \bar{c}$ *and either* $K = K_{\alpha_1}(c)$ *or* $K = K_{\alpha_2}(c)$.

If $K = K_{\alpha_1}(c)$, *Scenario IV, Fig.* 10, *the following composite waves are possible.*

(i) Combinations of cusp-components and plateaus at height $u = \alpha_1$ *for* $c_0 < c < c_1$.

(ii) Combinations of peak-components and plateaus at height $u = \alpha_1$ *for* $c = c_1$.

(iii) Waves u *with plateaus at height* $u = \alpha_1$ *and vanishing classical derivative on the preimage* $u^{-1}(\{\alpha_1\})$ *for* $c_1 < c \leq \bar{c}$.

In particular, there exist smooth and peaked multi-crested solutions with decay, cf. Fig. 11c *and* 11d, *and waves with plateaus at height* α_1, *cf. Fig.* 11a *and* 11b. *Moreover, there exist smooth and non-smooth* anti-compactons, *i.e. solitary waves of depression with compact support in the sense that they are constant equal to* α_1 *outside a finite interval, cf. Fig.* 11e.

If $K = K_{\alpha_2}(c)$, *Scenario VI, Fig.* 15, *the following composite waves are possible:*

(i) Combinations of anti-cusp-components and plateaus at height $u = \alpha_2$ *for* $c_0 < c \leq c_1$.

(ii) Combinations of anti-peak-components and plateaus at height $u = \alpha_2$ *for* $c_1 < c < \bar{c}$.

In particular, there exist anti-cuspcompactons *and* anti-peakompactons, *i.e. solitary cusped and peaked waves of depression with compact support, cf. Fig.* 17a.

Note that the classification of elementary traveling waves in Theorem 6.1 is exhaustive, while Theorems 6.2 and 6.3 merely highlight certain composite waves of special interest.

7. **Discussion and outlook.** In this paper we have studied traveling wave solutions of a highly nonlinear model equation for shallow water waves of large amplitude. Driven by the quest for new kinds of traveling waves which are not described by present day shallow water models, we resort to equation (1) which is a natural extension to moderate amplitude models such as the CH or the corresponding equation for the free surface [10]. The structure of the equation's higher order nonlinearities is responsible for the fact that the corresponding ordinary differential equation (5), which governs the traveling wave solutions of (1), becomes singular in potentially two points. This loss of uniqueness allows one to construct singular traveling wave solutions in $H^1_{\mathrm{loc}}(\mathbb{R})$ by combining various components of solution curves of the associated integrable planar system (8) corresponding to different level sets of the first integral. These components are smooth solutions of (8) defined on a (possibly bounded) subinterval of the real line. By gluing them together one finds traveling wave solutions, which are bounded and globally absolutely continuous with singularities at points where values α_i, $i \in \{1, 2\}$ – the roots of the quadratic polynomial $g(u)$ in (5) – are taken. The degree of this polynomial is two as a consequence of the presence of the third order cubic term in (1). This gives rise to entirely new types of traveling waves, whose wave profiles may exhibit singularities at two different heights. In particular, one obtains traveling waves where peaks and cusps form at both the wave crest and trough. These novel traveling wave solutions can not be described using CH type equations [19, 31, 32] since they lack a second singularity due to the absence of higher nonlinearities in higher order terms. Another novelty is that we can construct traveling waves involving non-symmetric

peaks whose slope differs from on either side of the crest or trough to the other. Moreover, recall that the CH solitary waves are monotone from crest to trough with a unique maximum. In contrast, here we have solitary waves whose profiles are non-monotonic as well as multi-crested peaked or smooth. Furthermore, we obtain negative smooth as well as anti-peaked and anti-cusped solitary waves with compact support, that is, the wave profile attains a constant value outside a finite interval. For comparison notice that it was shown to be impossible for moderate amplitude models to have peaks with compact support in [21]. Finally let us assert that we also recover all known smooth and singular traveling wave solutions of CH type equations.

It is known that the traveling wave solutions of models for moderate amplitude waves are symmetric with respect to their crest or trough as long as the solution conserves the energy of the corresponding planar system, see the discussions in [3, 18, 20]. This is true for equation (1) as well. Whether all symmetric solutions of (1) are necessarily traveling waves will be studied in a subsequent paper.

Regarding stability, we remark that smooth solitary as well as periodic traveling wave solutions of several shallow water equations have been shown to be orbitally stable, i.e. they are stable under small perturbations, which makes them physically detectable, see for example [2, 12, 14, 17, 30]. Moreover, singular traveling waves involving peaks, for instance the CH and DP peakons, are also known to be orbitally stable, cf. [11, 28, 29, 33]. This naturally raises the question whether traveling waves of (1) with peaked crests and troughs are stable in that sense as well. We expect the investigation of these issues to be quite involved since we are not aware of a Hamiltonian formulation for (1), and therefore the methods put forth to prove the aforementioned stability results in the moderate amplitude regime are not applicable here, cf. Remark 2.3. In this context it is worth pointing out that the stability of the traveling waves for these model equations is a shallow-water effect: while water waves are inherently unstable, the governing equations for water waves possess some vestige of these stability properties in the long-wave regime (see the discussion in the paper [13]). On the other hand, while a uniform train of plane waves of moderate amplitude in deep water is unstable to a small perturbation of other waves traveling in the same direction with nearly the same frequency (this is the Benjamin-Feir instability phenomenon, cf. [1]), many observed patterns of waves of moderate amplitude in deep water show no apparent instability; see the discussion in the paper [36].

Finally, we observe that it is possible to construct bounded continuous functions satisfying the properties (TW1) and (TW2) but not (TW3) of the characterization of traveling wave solutions given in Proposition 4.1. This can be achieved by using orbits indicated by dashed lines in the sketches of the phase portraits in Section 5. Such functions can not be interpreted as traveling wave solutions of (1) in the sense of Definition 2.1. In a forthcoming paper, we will investigate in which sense these functions can still be regarded as traveling solutions of (1) in Sobolev spaces $H^r_{\mathrm{loc}}(\mathbb{R})$ for certain suitable indices $r < 1$.

Acknowledgments. Both authors thank Armengol Gasull for valuable suggestions. We thank both referees for their helpful comments.

REFERENCES

[1] T. B. Benjamin and J. E. Feir, The disintegration of wavetrains in deep water, *J. Fluid Mech.*, **27** (1967), 417–430.

[2] J. L. Bona, P. E. Souganidis and W. Strauss, Stability and instability of solitary waves of Korteweg-de Vries type, *Proc. R. Soc. Lond., Ser. A, Math. Phys. Eng. Sci.*, **411** (1987), 395–412.
[3] G. Brüll, M. Ehrnström, A. Geyer and L. Pei, Symmetric solutions of evolutionary partial differential equations, *Nonlinearity*, **30** (2017), 3932–3950.
[4] R. Camassa and D. D. Holm, An integrable shallow water equation with peaked solitons, *Phys. Rev. Lett.*, **71** (1993), 1661–1664.
[5] A. Constantin, The trajectories of particles in Stokes waves, *Invent. Math.*, **166** (2006), 523–535.
[6] A. Constantin, An exact solution for equatorially trapped waves, *J. Geophys. Res.: Oceans*, **117** (2012), C05029.
[7] A. Constantin, Some nonlinear, equatorially trapped, nonhydrostatic internal geophysical waves, *J. Phys. Oceanogr.*, **44** (2014), 781–789.
[8] A. Constantin, *Nonlinear Water Waves with Applications to Wave-Current Interactions and Tsunamis*, CBMS-NSF Regional Conference Series in Applied Mathematics, **81**, SIAM Philadelphia, 2011.
[9] A. Constantin and J. Escher, Analyticity of periodic traveling free surface water waves with vorticity, *Ann. Math.*, **173** (2011), 559–568.
[10] A. Constantin and D. Lannes, The hydrodynamical relevance of the Camassa-Holm and Degasperis-Procesi equations, *Arch. Ration. Mech. Anal.*, **192** (2009), 165–186.
[11] A. Constantin and W. Strauss, Stability of peakons, *Commun. Pure Appl. Math.*, **53** (2000), 603–610.
[12] A. Constantin and W. Strauss, Stability of the Camassa-Holm solitons, *J. Nonlinear Sci.*, **12** (2002), 415–422.
[13] A. Constantin and W. Strauss, Stability properties of steady water waves with vorticity, *Comm. Pure Appl. Math.*, **60** (2007), 911–950.
[14] B. Deconinck and T. Kapitula, The orbital stability of the cnoidal waves of the Korteweg-de Vries equation, *Phys. Lett. Sect. A Gen. At. Solid State Phys.*, **374** (2010), 4018–4022.
[15] A. Degasperis and M. Procesi, Asymptotic integrability, In *A. Degasperis and G. Gaeta, editors, Symmetry and Perturbation Theory*, pages 23–37, World Scientific, Singapore, 1999.
[16] F. Dumortier, J. Llibre and J. C. Artés, *Qualitative Theory of Planar Differential Systems*, Springer, Berlin, 2006.
[17] N. Duruk Mutlubas and A. Geyer, Orbital stability of solitary waves of moderate amplitude in shallow water, *J. Differ. Equations*, **255** (2013), 254–263.
[18] M. Ehrnström, H. Holden and X. Raynaud, Symmetric waves are traveling waves, *Int. Math. Res. Not.*, **2009** (2009), 4578–4596.
[19] A. Gasull and A. Geyer, Traveling surface waves of moderate amplitude in shallow water, *Nonlinear Anal. Theory, Methods Appl.*, **102** (2014), 105–119.
[20] A. Geyer, Symmetric waves are traveling waves for a shallow water equation modeling surface waves of moderate amplitude, *J. Nonlinear Math. Phys.*, **22** (2015), 545–551.
[21] A. Geyer and V. Mañosa, Singular solutions for a class of traveling wave equations, *Nonlinear Anal. Real World Appl.*, **31** (2016), 57–76.
[22] J. Guggenheimer and P. Holmes, *Nonlinear Oscillations, Dynamical Systems, and Bifurcations of Vector Fields*, Springer, 1983.
[23] D. Henry, Equatorially trapped nonlinear water waves in a β-plane approximation with centripetal forces, *J. Fluid Mech.*, **804** (2016), R1, 11 pp.
[24] E. Hewitt and K. Stromberg, *Real and Abstract Analysis*, Springer-Verlag, New York-Heidelberg, 1975.
[25] V. M. Hur, Analyticity of rotational flows beneath solitary water waves, *Int. Math. Res. Not. IMRN*, **2012** (2012), 2550–2570.
[26] R. S. Johnson, Camassa-Holm, Korteweg-de Vries and related models for water waves, *J. Fluid Mech.*, **455** (2002), 63–82.
[27] D. J. Korteweg and G. de Vries, On the change of form of long waves advancing in a rectangular canal and on a new type of long stationary waves, *Phil. Mag.*, **39** (1895), 422–443.
[28] J. Lenells, A variational approach to the stability of periodic peakons, *J. Nonlinear Math. Phys.*, **11** (2004), 151–163.
[29] J. Lenells, Stability of periodic peakons, *Int. Math. Res. Not.*, **10** (2004), 485–499.
[30] J. Lenells, Stability for the periodic Camassa-Holm equation, *Math. Scand.*, **97** (2005), 188–200.

[31] J. Lenells, Traveling wave solutions of the Camassa-Holm equation, *J. Differ. Equ.*, **217** (2005), 393–430.
[32] J. Lenells, Traveling wave solutions of the Degasperis-Procesi equation, *J. Math. Anal. Appl.*, **306** (2005), 72–82.
[33] Z. Lin and Y. Liu, Stability of peakons for the Degasperis-Procesi equation, *Comm. Pure Appl. Math.*, **62** (2009), 125–146.
[34] T. Lyons, The pressure in a deep-water Stokes wave of greatest height, *J. Math. Fluid Mech.*, **18** (2016), 209–218.
[35] R. Quirchmayr, A new highly nonlinear shallow water wave equation, *J. Evol. Equations*, **16** (2016), 539–567.
[36] H. Segur, D. Henderson, J. Carter, J. Hammack, C.-M. Li, D. Pheiff and K. Socha, Stabilizing the Benjamin-Feir instability, *J. Fluid Mech.*, **539** (2005), 229–271.
[37] G. Teschl, *Ordinary Differential Equations and Dynamical Systems*, Graduate Studies in Mathematics **140**, AMS, Providence, RI, 2012.
[38] J. F. Toland, Stokes waves, *Topol. Methods Nonlinear Anal.*, **7** (1996), 1–48.
[39] E. Varvaruca and G. S. Weiss, The Stokes conjecture for waves with vorticity, *Ann. Inst. H. Poincaré Anal. Non Linéaire*, **29** (2012), 861–885.

Received August 2017; revised October 2017.

E-mail address: a.geyer@tudelft.nl
E-mail address: ronaldq@kth.se